

Group Network Hawkes Process

Guanhua Fang¹, Ganggang Xu², Haochen Xu³, Xuening Zhu³, and Yongtao Guan²

¹*Columbia University, USA*; ²*University of Miami, USA*

³*Fudan University, Shanghai, China*

Abstract

In this work, we study the event occurrences of individuals interacting in a network. To characterize the dynamic interactions among the individuals, we propose a group network Hawkes process (GNHP) model whose network structure is observed and fixed. In particular, we introduce a latent group structure among individuals to account for the heterogeneous user-specific characteristics. A maximum likelihood approach is proposed to simultaneously cluster individuals in the network and estimate model parameters. A fast EM algorithm is subsequently developed by utilizing the branching representation of the proposed GNHP model. Theoretical properties of the resulting estimators of group memberships and model parameters are investigated under both settings when the number of latent groups G is over-specified or correctly specified. A data-driven criterion that can consistently identify the true G under mild conditions is derived. Extensive simulation studies and an application to a data set collected from Sina Weibo are used to illustrate the effectiveness of the proposed methodology.

KEY WORDS: EM algorithm; Latent group structure; Multivariate Hawkes process; Network data analysis.

1 INTRODUCTION

Point process models have gained increasing popularity for modeling activities observed on various networks, examples include posting activities in online social networks (Sayyadi et al., 2009; Liu et al., 2012), corporation transactions in a financial network (Phua et al., 2010; Bacry et al., 2013), and neuron spikes in a brain network (Zhang et al., 2016). The main goal of this work is to develop a new modeling framework for random event times observed on a network consisting of heterogeneous nodes. While the proposed framework is applicable for the analysis of general

*Guanhua Fang and Ganggang Xu are joint first authors. Xuening Zhu (xueningzhu@fudan.edu.cn) is the corresponding author. Xuening Zhu is supported by the National Natural Science Foundation of China (nos. 11901105, 71991472, U1811461), the Shanghai Sailing Program for Youth Science and Technology Excellence (19YF1402700).

event time data, we describe our model in the context of a motivating dataset collected from Sina Weibo (the largest Twitter type social media platform in mainland China).

The dataset contains posting times from 2,038 users of Sina Weibo during the period from January 1st to January 15th, 2014. In Figure 1, we can see that posting patterns among users can be highly heterogeneous and complex. Firstly, we can see that the distribution of user post counts reveals great variability in users’ activities levels: while most users had less than 200 posts during the study period, a small portion of users were much more active. Secondly, the estimated overall intensity function of posting times aggregated over all users demonstrates the existence of apparent daily periodic patterns. Lastly, quantiles of gap times between a user’s posting time and the closest posting time from his/her connected friends and randomly picked non-friends are drastically different. In particular, the quantiles of gap times among friends are consistently smaller than those among the non-friends, suggesting that a user’s activities were heavily influenced by his/her friends.

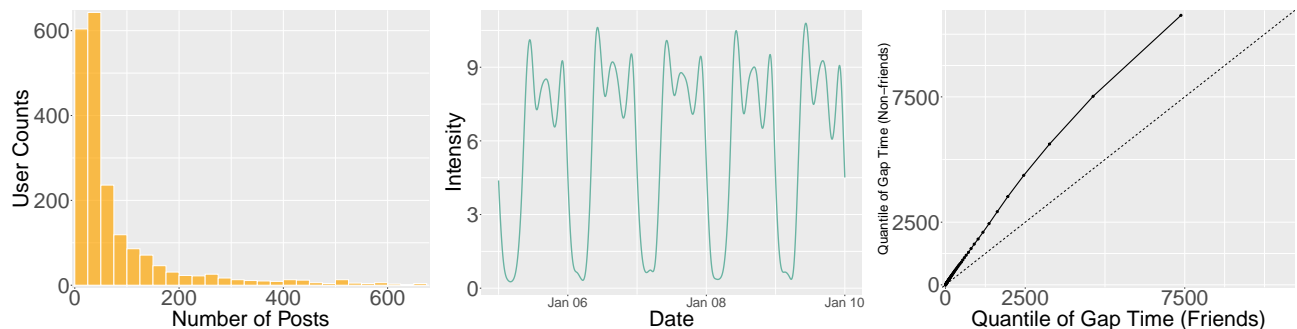


Figure 1: Left: histogram of users’ post counts. Middle: estimated overall intensity function of all users’ posting times. Right: QQ-plot of gap times among friends and among random picked non-friends.

A popular model for event time data such as that given in our motivating example is the so-called multivariate Hawkes process (Hawkes, 1971), which has been widely used to model event times of multiple types in a variety of fields, such as criminology (Linderman and Adams, 2014), finance (Bacry et al., 2013), information diffusion (Farajtabar et al., 2017), and social studies (Zhou et al., 2013; Fox et al., 2016). In the network setting, the event times at each node can be viewed as a realization from a component of the multivariate Hawkes process. For

such data, the first line of existing research aims at recovering the unknown network structure using the observed event time data, see, e.g., Zhou et al. (2013); Xu et al. (2016); Achab et al. (2018); Bacry et al. (2020). In contrast, another line of research takes the network structure as given knowledge and incorporates it into the modeling of the event time data. For instance, Fox et al. (2016) studied interactions among users in an E-mail network, where each user’s activities were influenced by others in the network. Farajtabar et al. (2017) developed a joint point process model for information diffusion and network evolution for an online social network such as Twitter or Sina Weibo. Zarezade et al. (2018) proposed to steer social activities to promote user engagement through a multivariate Hawkes process under a stochastic control algorithm. In the aforementioned work, the model parameters were assumed to be node-specific, and therefore the number of model parameters grows at least linearly with the number of nodes, which may be problematic if many nodes in the network produce only scarce even times, as observed in Figure 1 from the Weibo network. We defer to Section 2.4 for a more detailed comparison between the proposed model and existing works.

In this work, we propose a group network Hawkes process (GNHP) to model the network heterogeneity by introducing a latent group structure among the network nodes. We assume that nodes in the same group share similar node-wise characteristics and that interaction patterns between any two connected nodes are determined by their group memberships. For each latent group, we allow the background intensity to vary over time and use spline basis functions to approximate it nonparametrically. The proposed model is more parsimonious than existing models where all network nodes are considered as different (e.g., Fox et al., 2016; Farajtabar et al., 2017; Zarezade et al., 2018), but the latent group structure coupled with the observed network structure still allows us to build sufficiently flexible multivariate Hawkes process network models for many applications such as the social network posting data considered in Section 6. Furthermore, the proposed GNHP model admits an equivalent branching process structure which enables us to develop easily interpretable numerical measures to quantify interactions within the

network, see Section 2.3 for more details. The branching structure representation also allows us to develop a computationally efficient EM algorithm for model estimation, see Section 3.3. Lastly, the estimated group memberships enable us to cluster network nodes into several subgroups in a data-driven manner, which may offer further insights into the dynamics of the network activities. Therefore, from a practical point of view, the proposed GNHP model is an important addition to the existing toolbox for analyzing event time data observed on a network.

Our work also makes important theoretical contributions to the literature. Although there has been abundant literature on multivariate Hawkes process models, only a few have rigorously investigated asymptotic properties of the model estimators. Ogata (1978) studied the asymptotic property of the maximum likelihood estimator (MLE) for a univariate Hawkes process. For the multivariate Hawkes process, some concentration inequalities and asymptotic properties of moment-based estimators have been studied (e.g., Hansen et al., 2015; Chen et al., 2017; Cai et al., 2020). To the best of our knowledge, however, little is known about the limiting behaviors of the MLE for a high-dimensional multivariate Hawkes process such as the proposed GNHP. In this work, we establish the consistency results for the MLE of the model parameters and the latent group memberships in our proposed GNHP model, with the number of latent groups being possibly over-specified. When the number of latent groups is correctly specified, we establish the asymptotic normality of the MLE. Finally, we show that a likelihood-based information criterion (LIC) can be used to consistently select the number of latent groups. A similar theoretical framework has been considered in the panel data literature (Su et al., 2016; Liu et al., 2020), although the treatments of point process data and panel data are very different. In this sense, our work also bridges a gap between the point process literature and the panel data literature.

The rest of the article is organized as follows. In Section 2, we introduce the GNHP model together with its branching structure representation and compare the proposed model to existing works. In Section 3, we detail our estimation procedure, including the computationally efficient EM algorithm. Theoretical properties of resulting estimators are investigated in Section 4. Sim-

ulation results under different network settings are presented in Section 5. In Section 6, we apply the proposed model to the Sina Weibo dataset. The article is concluded with a brief discussion in Section 7. All technical details are left to online supplementary material.

2 GROUP NETWORK HAWKES PROCESS

2.1 Background on Hawkes Process

Hawkes process is a self-exciting process proposed by Hawkes (1971). Denote by $0 \leq t_1 \leq t_2 \leq \dots \leq t_n \leq T$ a realization of a temporal point process defined in $[0, T]$ and let $N(t) = \sum_{k=1}^n I(t_k < t)$ be the associated counting process, where $I(\cdot)$ is an indicator function. Let $\mathcal{H}_t = \{t_k : t_k < t\}$ be the process history up to time t , conditioned on which the conditional intensity function of a point process is defined as $\lambda(t|\mathcal{H}_t) = \lim_{\Delta \rightarrow 0} \Delta^{-1} \mathbb{E}[N(t + \Delta) - N(t)|\mathcal{H}_t]$. The classical Hawkes process model (Hawkes, 1971) assumes that $\lambda(t|\mathcal{H}_t)$ takes the form

$$\lambda(t|\mathcal{H}_t) = \mu + \sum_{t_k < t} f(t - t_k), \quad (1)$$

where $\mu > 0$ is a background rate of events and $f(\cdot)$ is a non-negative triggering function. The Hawkes process is considered as “self-exciting” since the past events in \mathcal{H}_t contribute to the instantaneous intensity $\lambda(t|\mathcal{H}_t)$ at time t through $f(\cdot)$. The triggering function controls the dependence range and strength between the intensity at time t and the past events, and popular choices include the exponential kernel (Hawkes, 1971) and the power-law kernel (Ogata, 1988).

Notations. For a vector $\mathbf{v} = (v_1, \dots, v_p)^\top \in \mathbb{R}^p$, let $\|\mathbf{v}\|_2 = (\sum_{i=1}^p v_i^2)^{1/2}$ and $\|\mathbf{v}\|_\infty = \max_j |v_j|$ denote the L_2 -norm and the infinity norm of \mathbf{v} , respectively. For a function $h(t) \in \mathbb{R}^1$ with $t \in [0, T]$, define $\|h(\cdot)\|_T = \{T^{-1} \int_0^T h(t)^2 dt\}^{1/2}$ and $\|h(\cdot)\|_\infty = \sup_{t \in [0, T]} |h(t)|$. For a matrix $\mathbf{H} = (h_{ij}) \in \mathbb{R}^{m \times n}$, define the row norm $\|\mathbf{H}\|_\infty = \max_i (\sum_j |h_{ij}|)$. For any set \mathcal{S} , define $\mathcal{S}^n = \{\mathbf{v} = (v_1, \dots, v_n)^\top : v_i \in \mathcal{S}\}$ as collection of vectors of length n , whose elements are in \mathcal{S} . Finally, we denote $[G] = \{1, \dots, G\}$ and $\mathbf{1} = (1, \dots, 1)^\top$.

2.2 Network Hawkes Process with Latent Group Structures

In this section, we extend the classical Hawkes process model to the network setting with a latent group structure. Consider a network with m nodes, where the relationships among the nodes are characterized by an adjacency matrix $A = (a_{ij}) \in \mathbb{R}^{m \times m}$, with $a_{ij} = 1$ indicating that the i th node follows the j th node and $a_{ij} = 0$ suggesting otherwise. By convention, we do not allow self-connected nodes, i.e., $a_{ii} = 0$. To account for potential heterogeneity in the network nodes, we assume that the nodes in the network belong to G homogeneous latent groups in the sense that nodes within the same group share the same node-specific characteristics and interactions with nodes from other groups.

Denote $\mathcal{G} = (g_1, \dots, g_m)^\top \in \mathbb{R}^m$ as the latent group membership vector of all nodes, where $g_i \in [G]$ for $i = 1, \dots, m$. For the i th node, let $0 \leq t_{i1} \leq t_{i2} \leq \dots \leq t_{in_i} \leq T$ be the observed event times, where n_i is the total number of events. The associated counting process for the i th node can subsequently be defined as $N_i(t) = \sum_{k=1}^{n_i} I(t_{ik} \leq t)$. Given the group membership vector \mathcal{G} and event history $\mathcal{H}_t = \{t_{ik} : t_{ik} < t; 1 \leq k \leq n_i, 1 \leq i \leq m\}$, our proposed GNHP model assumes that the conditional intensity function for the i th node is of the form

$$\lambda_i(t|\mathcal{G}, \mathcal{H}_t) = \mu_{g_i}(t) + \beta_{g_i} \sum_{t_{ik} < t} f_b(t - t_{ik}; \eta_{g_i}) + \sum_{j=1}^m \phi_{g_i g_j} \frac{a_{ij}}{d_i} \sum_{t_{jl} < t} f_b(t - t_{jl}; \gamma_{g_i}), \quad (2)$$

for $i = 1, \dots, m$, where $\mu_g(\cdot)$ is a baseline intensity function, $f_b(\cdot; \eta)$ is a triggering function governed by the parameter η , $d_i = \sum_{j=1}^m a_{ij}$ is the out-degree for node i , and $\{\beta_g \geq 0, \gamma_g \geq 0, \eta_g \geq 0, \phi_{gg'} \geq 0\}$ are unknown group-level parameters, for $g, g' = 1, \dots, G$. Following Hansen et al. (2015) and Chen et al. (2017), we assume the support of $f_b(t; \gamma)$ is $[0, b]$. For example, $f_b(\cdot; \gamma)$ can be a truncated exponential kernel of the form

$$f_b(t; \gamma) = \gamma [1 - \exp(-b\gamma)]^{-1} \exp(-\gamma t) I(t \leq b), \quad \text{for any } t \geq 0. \quad (3)$$

In our theoretical investigation, we allow the truncation range $b \rightarrow \infty$ as $m, T \rightarrow \infty$. For identifiability of the parameters β_g 's and $\phi_{gg'}$'s, we assume that $\int_0^\infty f_b(t; \gamma) dt = 1$ for any given

γ . In addition, we assume that $\|\partial^k f_b(\cdot; \gamma)/\partial \gamma^k\|_\infty < \infty$ for $1 \leq k \leq 3$.

The proposed conditional intensity in (2) can be decomposed into the following three parts.

- **BASELINE INTENSITY** $\mu_{g_i}(t)$. This describes the overall activity pattern of the node i .
- **MOMENTUM INTENSITY** $\beta_{g_i} \sum_{t_{ik} < t} f_b(t - t_{ik}; \eta_{g_i})$. It models “self-exciting” influence of its own past events on the occurrence of a new event at t at the node i .
- **NETWORK INTENSITY** $d_i^{-1} \sum_{j=1}^m \phi_{g_i g_j} a_{ij} \sum_{t_{jl} < t} f_b(t - t_{jl}; \gamma_{g_i})$. This models influences from past events of other nodes on the likelihood of a new event occurring at t at the node i .

The out-degree d_i is used to prevent the inflation of the *Network Intensity* when $d_i \rightarrow \infty$, which is commonly done in literature (Lee, 2004; Liu, 2014; Zhu et al., 2017; Cohen-Cole et al., 2018; Zhu et al., 2019b). The $\phi_{g_i g_j}$ ’s in the *Network Intensity* represent the average network influences from the connected nodes on the i th node. Finally, we remark that the triggering functions in the *Momentum Intensity* and the *Network Intensity* do not necessarily share the same form.

The network dependence of the proposed GNHP can be characterized by the transition matrix $\mathbf{B} = (b_{ij}) \in \mathbb{R}^{m \times m}$, where $b_{ij} = \phi_{g_i g_j} d_i^{-1} a_{ij} + \beta_{g_i} I(i = j)$, for $i, j = 1, \dots, m$. Detailed properties of \mathbf{B} will be further explored in the next subsection based on the following assumption.

Assumption 1. Assume $\|\mathbf{B}\|_\infty \leq c_B < 1$, where c_B is a positive constant.

Assumption 1 is a sufficient condition for stability of a multivariate Hawkes process and has been widely used in the literature, see, e.g., Hansen et al. (2015); Chen et al. (2017). In the next subsection, we show that for the GNHP model, it is a sufficient condition to ensure that the expected number of offspring events triggered by a parent event at any network node is finite.

2.3 Branching Structure of the GNHP Model

Hawkes and Oakes (1974) provides an equivalent branching structure representation for the classical Hawkes process (1), which classifies the observed events into two disjoint processes:

a *parent Poisson process* with a rate μ , and *offspring processes* triggered by past events. The branching structure of the classical Hawkes process is illustrated in the left panel of Figure 2.

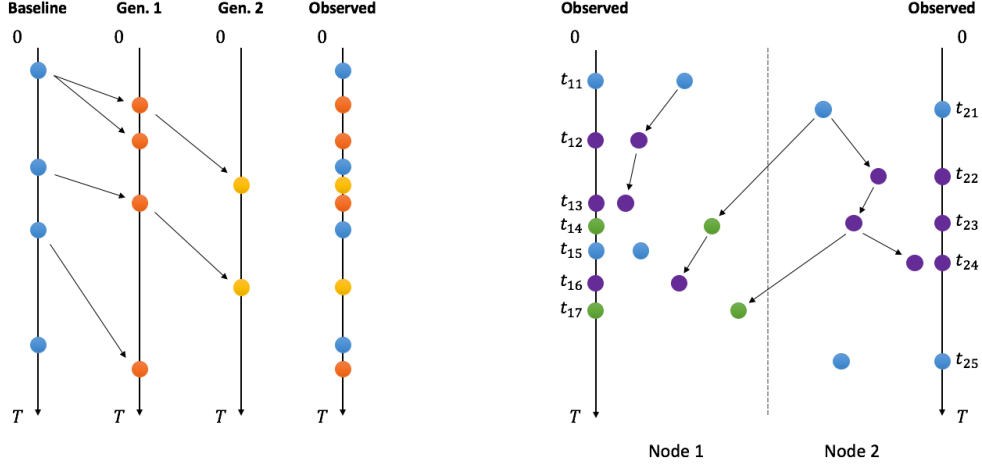


Figure 2: Branching structures of the classical Hawkes process (left) and the GNHP model (right). Left panel: parent events (blue circle) and two generations of offspring events; Right panel: a two-node network where Node 1 follows Node 2. The blue circles represent parent events from both nodes, the purple circles indicate event times triggered by their own past events for Nodes 1 and 2, the green circles are the event times in Node 1 that are triggered by past events from Node 2.

Following Rasmussen (2013) and Halpin et al. (2013), a branching structure representation can be derived for the GNHP model by treating the aggregated point process from all network nodes, denoted by N^{pool} , as a marked point process defined on $[0, T]$, with the mark for any $t \in N^{\text{pool}}$ being the node index where the event occurs. Specifically, event times in N^{pool} can be categorized into two types: the parent events and the offspring events. Denote $\mathcal{M}_i^{\text{parent}}$ as the set of all parent events from the node i and let $\mathcal{M}_{ik}^{\text{fam}} = \mathcal{M}_{ik}^{\text{off}} \cup \{t_{ik}\}$, where $\mathcal{M}_{ik}^{\text{off}}$ is the set of offspring events generated from a parent event $t_{ik} \in \mathcal{M}_i^{\text{parent}}$. We emphasize that $\mathcal{M}_{ik}^{\text{fam}}$ may contain event times from other nodes due to the interactions within the network. The branching structure is then defined as follows.

1. For any $1 \leq i \leq m$, the parent events $\mathcal{M}_i^{\text{parent}}$ follows a Poisson process with an intensity $\mu_{g_i}(t)$, and all Poisson processes are independent.
2. Each parent event $t_{ik} \in \mathcal{M}_i^{\text{parent}}$ generates a set of offspring events $\mathcal{M}_{ik}^{\text{off}}$, and all resulting $\mathcal{M}_{ik}^{\text{fam}}$'s are independent. Event times in each $\mathcal{M}_{ik}^{\text{fam}}$ are generated recursively as follows.

- (a) Generation 0, denoted as $\mathcal{M}_{ik}^{gen_0}$, consists of only t_{ik} , i.e., $\mathcal{M}_{ik}^{gen_0} = \{t_{ik}\}$.
- (b) Having generated offspring event times up to n generations, $\mathcal{M}_{ik}^{gen_0}, \dots, \mathcal{M}_{ik}^{gen_n}$, each event time in $\mathcal{M}_{ik}^{gen_n}$ generates a series of event times of the $n+1$ generation. Specifically, suppose $t_{jl} \in \mathcal{M}_{ik}^{gen_n}$ is an event time located in the j th node, then on the time interval $[t_{jl}, T]$, it generates (i) a Poisson process with intensity $\beta_{g_j} f_b(t - t_{jl}; \eta_{g_j})$ on the node j ; and (ii) a Poisson process with intensity $\phi_{g_{i'}g_j} d_{i'}^{-1} f_b(t - t_{jl}; \gamma_{g_{i'}})$ on the node i' for any $1 \leq i' \leq m$ such that $a_{i'j} = 1$. All Poisson processes are independent.
- (c) Obtain $\mathcal{M}_{ik}^{fam} = \cup_{n=0}^{\infty} \mathcal{M}_{ik}^{gen_n}$.

Figure 2 illustrates the branching structure of the GNHP model with a network of two nodes.

Theorem 1. Denote by $\#_i(\mathcal{S})$ the total number of events occurring at a subset of network nodes $\mathcal{S} \subset \{1, \dots, m\}$ that are offspring events of a parent event originated from the i th node on $[0, \infty)$. Then under Assumption 1, one has that

$$E[\#_i(\mathcal{S})] = \mathbf{e}_{\mathcal{S}}^{\top} (\mathbf{I} - \mathbf{B})^{-1} \mathbf{e}_i, \text{ for any } 1 \leq i \leq m, \quad (4)$$

where $\mathbf{e}_{\mathcal{S}}$ is a vector with 1 for entries whose indexes are in \mathcal{S} and 0 elsewhere, and $\mathbf{e}_i = \mathbf{e}_{\{i\}}$.

The proof is given in the online Supplement. Theorem 1 provides a useful tool to quantify the network interactions. Examples include

- **NODE-TO-NODE INFLUENCE:** the (j, i) th entry of $(\mathbf{I} - \mathbf{B})^{-1}$ gives the average number of events at node j that are triggered by a parent event at the i th node (set $\mathcal{S} = \{j\}$).
- **NODE-TO-NETWORK INFLUENCE:** by setting $\mathcal{S} = \{1, \dots, m\}$, we obtain the sum of the i th column of $(\mathbf{I} - \mathbf{B})^{-1}$ as the average number of events in the entire network that are directly/indirectly triggered by a parent event at the i th node, i.e., $E\{\#_i(\mathcal{S})\} = E\{|\mathcal{M}_{ik}^{fam}|\}$.
- **DYNAMIC GROUP-TO-GROUP INFLUENCE:** Let \mathcal{S}_g be the collection of node indexes in group g . Denote $\#(\mathcal{S}_g, \mathcal{S}_{g'}, [t_1, t_2])$ as the total number of events from group g' triggered by

parent events from group g occurring within $[t_1, t_2]$, which reflects the influential power of group g on group g' . Based on Theorem 1, it can be verified that $E\left\{\#(\mathcal{S}_g, \mathcal{S}_{g'}, [t_1, t_2])\right\} = \mathbf{e}_{\mathcal{S}_{g'}}^\top (\mathbf{I} - \mathbf{B})^{-1} \mathbf{e}_{\mathcal{S}_g} \int_{t_1}^{t_2} \mu_g(t) dt$. We can subsequently define the limiting case as follows

$$\text{GIF}_{gg'}(t) = \lim_{\Delta \rightarrow 0} \Delta^{-1} E\left\{\#(\mathcal{S}_g, \mathcal{S}_{g'}, [t, t + \Delta])\right\} = \mathbf{e}_{\mathcal{S}_{g'}}^\top (\mathbf{I} - \mathbf{B})^{-1} \mathbf{e}_{\mathcal{S}_g} \mu_g(t), \quad t \in [0, T], \quad (5)$$

which is more convenient for graphical illustrations.

2.4 Comparisons with Existing Literature

There has been much work on multivariate Hawkes process (e.g., Zhou et al., 2013; Bacry et al., 2013; Chen et al., 2017), and models for the conditional intensity can be generally expressed as

$$\lambda_i(t|\mathcal{G}, \mathcal{H}_t) = \mu_i + \sum_{j=1}^m \sum_{t_{jl} < t} \zeta_{ij}(t - t_{jl}), \quad i = 1, \dots, m, \quad (6)$$

where μ_i is the background rates at the node i and $\zeta_{ij}(\cdot)$ is some transition function between the node j and the node i . Key differences among existing multivariate Hawkes process models center around constructions of $\zeta_{ij}(\cdot)$'s. A popular modeling strategy is to assume that

$$\zeta_{ij}(\cdot) = \theta_{ij} f(\cdot; \gamma), \quad i, j = 1, \dots, m, \quad (7)$$

where $f(\cdot; \gamma)$ is of some parametric form. Such a model involves a total number of $O(m^2)$ parameters, restricting its suitability to applications with a relatively small m (e.g., Bacry et al., 2013). When modeling a network with a large number of nodes, one needs to impose some sparse structure on θ_{ij} 's, where a nonzero θ_{ij} implies that the node i is directly influenced by the node j . The estimated θ_{ij} 's may help recover the latent network structure (e.g., Zhou et al., 2013; Xu et al., 2016; Bacry et al., 2020). While most existing work in this direction lack rigorous theory, there has been some recent work on theoretical investigations of such models when m is diverging, see, e.g., Hansen et al. (2015), Chen et al. (2017) and Cai et al. (2020).

One drawback of the network structure estimation based on the sparsity assumption is the lack

of a clear interpretation of the estimated multivariate Hawkes model. To overcome this drawback, there has been another line of research that focuses on parameterization of (7) utilizing a known network structure, see, e.g., Fox et al. (2016), Farajtabar et al. (2017), and Zarezade et al. (2018). For instance, Fox et al. (2016) models email communications in a network by assuming $\zeta_{ij}(t) = \theta_i a_{ij} \gamma_i \exp(-\gamma_i t)$, where $A = (a_{ij})$ is the adjacency matrix of the observed network, and θ_i 's and γ_i 's are unknown parameters. As a result, the total number of unknown parameters is reduced to $O(m)$ from $O(m^2)$ in model (7). Similar but more complex models were studied in Farajtabar et al. (2017) and Zarezade et al. (2018).

Our proposed GNHP model falls into the second line of research with four distinct features: (a) the background intensities $\mu_i(\cdot)$'s are allowed to be time-varying and nonparametrically approximated using spline basis functions, which provides greater modeling flexibility. (b) the *Momentum Intensity* in model (2) has a clear interpretation given the network structure. (c) the latent group structure imposed on network nodes not only accounts for commonly observed network heterogeneity in a natural way but also effectively reduces the number of parameters. (d) the estimated group memberships for network nodes may provide further insights on the network activities using various influence measures discussed in Section 2.3.

3 MODEL ESTIMATION

3.1 Background Intensity Approximation

As illustrated in Figure 1, human activities such as social media posting often exhibit periodic patterns. We, therefore, assume that the background intensity of a given node takes a periodic form. Specifically, we assume that there exists a finite $\omega > 0$ such that for any $g \in [G]$, $\mu_g(t) = \mu_g(t + l\omega)$, $t \in [0, T - l\omega]$, $l = 0, 1, 2, \dots$. For our social network posting example, it is natural to choose $\omega = 1$ day (or 24 hours) to account for periodic daily posting behaviors. Without assuming any restrictive parametric form for $\mu_g(\cdot)$'s, we approximate $\mu_g(\cdot)$ using periodic

spline basis functions. Let $\mathbf{k}_{n_{\text{kt}}}(\cdot) = (k_1(\cdot), \dots, k_{n_{\text{kt}}}(\cdot))^\top$ be a collection of n_{kt} basis functions defined on $[0, \omega]$ and $\mathbf{x}_{n_{\text{kt}}}(t) = \sqrt{n_{\text{kt}}} \mathbf{k}_{n_{\text{kt}}}(t - \lfloor t/\omega \rfloor \omega)$ for any $t \in [0, T]$, where $\lfloor a \rfloor$ is the largest integer less than or equal to a , then $\mu_g(\cdot)$ is approximated by

$$\mu_g(t) = \mathbf{w}_g^\top \mathbf{x}_{n_{\text{kt}}}(t), \quad t \in [0, T], \quad (8)$$

where \mathbf{w}_g , $g = 1, \dots, G$, are the coefficient vectors that need to be estimated. For our theoretical investigation, we require the following assumption for the spline basis functions.

Assumption 2. Assume that there exists a constant $R > 0$ such that $k_1(\cdot), \dots, k_{n_{\text{kt}}}(\cdot)$ satisfy: (a) $\|k_j(\cdot)\|_\infty \leq R$ and $\int_0^\omega k_j(t)dt = O(n_{\text{kt}}^{-1})$; (b) $\int_0^\omega k_j(t)k_{j+l}(t)dt = O(n_{\text{kt}}^{-1})$, and $k_j(t)k_{j+l}(t) = 0$ for $l > J$ and any $t \in [0, \omega]$, where $J \geq 0$ is a finite integer. Denote by $\mu_g^0(\cdot)$ the true background function of group g , and assume that for some constant $r > 0$, it holds that

$$\max_{1 \leq g \leq G} \inf_{\mathbf{w}_g \in \mathbb{R}^{n_{\text{kt}}}, \|\mathbf{w}_g\|_\infty \leq R/\sqrt{n_{\text{kt}}}} \|\mu_g^0(\cdot) - \mathbf{w}_g^\top \mathbf{x}_{n_{\text{kt}}}(\cdot)\|_\infty = O(n_{\text{kt}}^{-r}). \quad (9)$$

Assumption 2 requires that the true background intensity functions can be approximated sufficiently well by a linear combination of spline basis functions, which is mild for many spline families. In our numerical examples, we choose $k_1(\cdot), \dots, k_{n_{\text{kt}}}(\cdot)$ as the r th-order B-spline basis functions with equally spaced knots on $[0, \omega]$, which meet Assumption 2 (Zhou et al., 1998).

3.2 Maximum Likelihood Estimation

For any $g \neq g'$, denote $\mathbb{W} \subset \mathbb{R}^{n_{\text{kt}}}$, $\Theta \subset \mathbb{R}^3$ and $\Phi \subset \mathbb{R}^+$ as the parameter spaces for parameters in \mathbf{w}_g , $\theta_g = (\beta_g, \eta_g, \gamma_g)^\top$, and $\phi_{gg'}$'s, respectively. Here \mathbb{R}^+ denotes $[0, \infty)$. Denote by $\mathbb{G} \equiv [G]^m$ as the parameter space for the membership vector $\mathcal{G} = (g_1, \dots, g_m)^\top$. For our theoretical investigation, we impose the following assumption on the parameter spaces.

Assumption 3. There exist $R > 0, C > 0$ such that (a) $\sup_{\mathbf{w} \in \mathbb{W}} \|\mathbf{w}\|_\infty \leq R/\sqrt{n_{\text{kt}}}$ and $\inf_{\mathbf{w} \in \mathbb{W}} \inf_{t \in [0, T]} \mathbf{w}^\top \mathbf{x}_{n_{\text{kt}}}(t) \geq C$; (b) $\sup_{\theta \in \Theta} \|\theta\|_\infty \leq R$; and (c) $\sup_{\phi \in \Phi} |\phi| \leq R$.

Denote $\mathcal{N}_i = \{j : a_{ij} = 1\}$ as the index set of the d_i neighboring nodes of the node i ,

$\mathcal{G}_i = (g_{j_1}, \dots, g_{j_{d_i}})^\top$ as the corresponding group membership vector of all nodes in \mathcal{N}_i , and the re-scaled interaction parameter $\boldsymbol{\varphi}_{g_i, \mathcal{G}_i} = d_i^{-1/2}(\phi_{g_i g_{j_1}}, \dots, \phi_{g_i g_{j_{d_i}}})^\top$, $i = 1, \dots, m$. The term $d_i^{-1/2}$ used in $\boldsymbol{\varphi}_{g_i, \mathcal{G}_i}$ is convenient for our theoretical study but is of no particular importance. It is straightforward to see that the conditional intensity (2) of the node i only depends on $\mu_{g_i}(\cdot) = \mathbf{w}_{g_i}^\top \mathbf{x}_{n_{kt}}(\cdot)$, $\boldsymbol{\theta}_{g_i}$ and $\boldsymbol{\varphi}_{g_i, \mathcal{G}_i}$, and therefore can be rewritten as

$$\lambda_i(t|\mathbf{w}_{g_i}, \boldsymbol{\theta}_{g_i}, \boldsymbol{\varphi}_{g_i, \mathcal{G}_i}, \mathcal{H}_t) = \mathbf{w}_{g_i}^\top \mathbf{x}_{n_{kt}}(t) + \beta_{g_i} \sum_{t_{ik} < t} f_b(t - t_{ik}; \eta_{g_i}) + \sum_{j=1}^m \frac{a_{ij} \phi_{g_i g_j}}{d_i} \sum_{t_{jl} < t} f_b(t - t_{jl}; \gamma_{g_i}), \quad (10)$$

for $i = 1, \dots, m$. Denote the parameter vectors $\underline{\mathbf{w}} = (\mathbf{w}_1^\top, \dots, \mathbf{w}_G^\top)^\top \in \mathbb{W}^G$, $\underline{\boldsymbol{\theta}} = (\boldsymbol{\theta}_1^\top, \dots, \boldsymbol{\theta}_G^\top)^\top \in \boldsymbol{\Theta}^G$, and $\underline{\boldsymbol{\phi}} = (\phi_{11}, \dots, \phi_{1G}, \phi_{21}, \dots, \phi_{G,G})^\top \in \boldsymbol{\Phi}^{G^2}$. Consequently, the log-likelihood function (divided by mT) of the proposed GNHP can be shown to have the form

$$\ell(\underline{\mathbf{w}}, \underline{\boldsymbol{\theta}}, \underline{\boldsymbol{\phi}}, \mathcal{G}|\mathcal{H}_T) = \frac{1}{m} \sum_{i=1}^m \ell_i(\mathbf{w}_{g_i}, \boldsymbol{\theta}_{g_i}, \boldsymbol{\varphi}_{g_i, \mathcal{G}_i}|\mathcal{H}_T), \quad \text{where} \quad (11)$$

$$\ell_i(\mathbf{w}_{g_i}, \boldsymbol{\theta}_{g_i}, \boldsymbol{\varphi}_{g_i, \mathcal{G}_i}|\mathcal{H}_T) = \frac{1}{T} \left\{ \sum_{k=1}^{n_i} \log [\lambda_i(t_{ik}|\mathbf{w}_{g_i}, \boldsymbol{\theta}_{g_i}, \boldsymbol{\varphi}_{g_i, \mathcal{G}_i}, \mathcal{H}_{t_{ik}})] - \int_0^T \lambda_i(t|\mathbf{w}_{g_i}, \boldsymbol{\theta}_{g_i}, \boldsymbol{\varphi}_{g_i, \mathcal{G}_i}, \mathcal{H}_t) dt \right\}.$$

For ease of presentation, from now on, we denote $\underline{\boldsymbol{\psi}} = (\underline{\mathbf{w}}^\top, \underline{\boldsymbol{\theta}}^\top, \underline{\boldsymbol{\phi}}^\top, \mathcal{G}^\top)^\top$ and the MLE of the parameters are then obtained by

$$\hat{\underline{\boldsymbol{\psi}}} \equiv \left(\hat{\underline{\mathbf{w}}}^\top, \hat{\underline{\boldsymbol{\theta}}}^\top, \hat{\underline{\boldsymbol{\phi}}}^\top, \hat{\mathcal{G}}^\top \right)^\top = \underset{\underline{\mathbf{w}}, \underline{\boldsymbol{\theta}}, \underline{\boldsymbol{\phi}}, \mathcal{G}}{\operatorname{argmax}} \ell(\underline{\mathbf{w}}, \underline{\boldsymbol{\theta}}, \underline{\boldsymbol{\phi}}, \mathcal{G}|\mathcal{H}_T), \quad \text{where } \hat{\mathcal{G}} = (\hat{g}_1, \dots, \hat{g}_m)^\top. \quad (12)$$

3.3 An EM Algorithm

Direct maximization of (11) is a non-convex problem with a large number of parameters, which can be computationally challenging. In this subsection, we propose a more efficient algorithm by taking advantage of the branching structure given in Section 2.3.

For the k th event of the i th node that occurs at time t_{ik} , define a latent random variable $Z_{ik} = (j, l)$, where $j = l = 0$ indicates that the k th event is a parent event, and otherwise it means the k th event is triggered by the l th event from the j th node at time point t_{jl} . Given $\mathbf{Z}_i = (Z_{i1}, \dots, Z_{i n_i})^\top$, all event times of the i th node can be categorized into three types:

1. Parent events with $Z_{ik} = (0, 0)$, which constitute a realization of a Poisson process on $[0, T]$ with an intensity $\mu_{g_i}(\cdot)$. The log-likelihood can then be written as

$$\ell_{\text{br},i}^{(1)}(\mathbf{w}_{g_i}|\mathcal{H}_T, \mathbf{Z}_i) = \sum_{k=1}^{n_i} I[Z_{ik} = (0, 0)] \log [\mathbf{w}_{g_i}^\top \mathbf{x}_{n_{\text{kt}}}(t_{ik})] - \int_0^T [\mathbf{w}_{g_i}^\top \mathbf{x}_{n_{\text{kt}}}(t)] dt. \quad (13)$$

2. All t_{ik} 's triggered by a past event of the node i , i.e., $Z_{ik} = (i, l)$ for some $1 \leq l < k$, which form a realization of a Poisson process on $[t_{il}, T]$ with an intensity $\beta_{g_i} f_b(t - t_{il}; \eta_{g_i})$ for any $t \in [t_{il}, T]$. The joint log-likelihood of all such events is of the form

$$\ell_{\text{br},i}^{(2)}(\beta_{g_i}, \eta_{g_i}|\mathcal{H}_T, \mathbf{Z}_i) = \sum_{l=1}^{n_i-1} \left\{ \sum_{k=l+1}^{n_i} I[Z_{ik} = (i, l)] \log [\beta_{g_i} f_b(t_{ik} - t_{il}; \eta_{g_i})] - \beta_{g_i} \int_{t_{il}}^T f_b(t - t_{il}; \eta_{g_i}) dt \right\}. \quad (14)$$

3. All t_{ik} 's triggered by a past event of a node $j \in \mathcal{N}_i$, i.e., $Z_{ik} = (j, l)$ for some $1 \leq l < n_j$ and $j \in \mathcal{N}_i$, which form a realization of a Poisson process on $[t_{jl}, T]$ with an intensity $d_i^{-1} \phi_{g_i g_j} f_b(t - t_{jl}; \gamma_{g_i})$ for any $t \in [t_{jl}, T]$. The joint log-likelihood of all such events becomes

$$\ell_{\text{br},i}^{(3)}(\gamma_{g_i}, \varphi_{g_i, \mathcal{G}_i}|\mathcal{H}_T, \mathbf{Z}_i) = \sum_{j \in \mathcal{N}_i} \sum_{l=1}^{n_j} \left\{ \sum_{k=1}^{n_i} I[Z_{ik} = (j, l)] \log \left[\frac{\phi_{g_i g_j}}{d_i} f_b(t_{ik} - t_{jl}; \gamma_{g_i}) \right] - \frac{\phi_{g_i g_j}}{d_i} \int_{t_{jl}}^T f_b(t - t_{jl}; \gamma_{g_i}) dt \right\}. \quad (15)$$

Consequently, when $\mathbf{Z} = (\mathbf{Z}_1^\top, \dots, \mathbf{Z}_m^\top)^\top$ is observed, by the branching structure given in Section 2.3, the complete log-likelihood for the proposed GNHP is then of the form

$$\ell_{\text{br}} \left(\underline{\psi} | \mathcal{H}_T, \mathbf{Z} \right) = \sum_{i=1}^m \left[\ell_{\text{br},i}^{(1)}(\mathbf{w}_{g_i}|\mathcal{H}_T, \mathbf{Z}_i) + \ell_{\text{br},i}^{(2)}(\beta_{g_i}, \eta_{g_i}|\mathcal{H}_T, \mathbf{Z}_i) + \ell_{\text{br},i}^{(3)}(\gamma_{g_i}, \varphi_{g_i, \mathcal{G}_i}|\mathcal{H}_T, \mathbf{Z}_i) \right]. \quad (16)$$

The MLE (12) can then be obtained by an EM algorithm using the complete likelihood (16), and similar approaches have been used in Veen and Schoenberg (2008); Halpin et al. (2013); Fox et al. (2016). Since the likelihood (11) is non-convex, the initial values of the group memberships and model parameters are of crucial importance. We propose to use a combination of the K-means algorithm and a stochastic EM algorithm to generate sensible initial values. The details are given in the Section A of the supplementary material.

3.4 Membership Refinement

The MLE (12) maximizes the overall log-likelihood function (11), but not necessarily each node-specific likelihood $\ell_i(\mathbf{w}_g, \boldsymbol{\theta}_g, \boldsymbol{\varphi}_{g, \mathcal{G}_i} | \mathcal{H}_T)$, $i = 1, \dots, m$. As a result, if $\ell_i(\widehat{\mathbf{w}}_{\widehat{g}_i}, \widehat{\boldsymbol{\theta}}_{\widehat{g}_i}, \widehat{\boldsymbol{\varphi}}_{\widehat{g}_i, \widehat{\mathcal{G}}_i} | \mathcal{H}_T)$ is too low for a given i , its membership estimate \widehat{g}_i may be incorrect. To address this issue, in this subsection, we propose a refinement strategy for the membership estimates.

One way to check whether the estimated \widehat{g}_i results in a too small $\ell_i(\widehat{\mathbf{w}}_{\widehat{g}_i}, \widehat{\boldsymbol{\theta}}_{\widehat{g}_i}, \widehat{\boldsymbol{\varphi}}_{\widehat{g}_i, \widehat{\mathcal{G}}_i} | \mathcal{H}_T)$ is to compare to the profile likelihood $\ell_i^p(g | \mathcal{H}_T) = \sup_{\boldsymbol{\varphi}_i \in \Phi_i} \ell_i(\widehat{\mathbf{w}}_g, \widehat{\boldsymbol{\theta}}_g, \boldsymbol{\varphi}_i | \mathcal{H}_T)$, where Φ_i is a parameter space of dimension d_i . If for some \widetilde{g} such that $\ell_i^p(\widetilde{g} | \mathcal{H}_T)$ is much greater than $\ell_i(\widehat{\mathbf{w}}_{\widehat{g}_i}, \widehat{\boldsymbol{\theta}}_{\widehat{g}_i}, \widehat{\boldsymbol{\varphi}}_{\widehat{g}_i, \widehat{\mathcal{G}}_i} | \mathcal{H}_T)$, it may be a sign to relabel the node i to group \widetilde{g} . Furthermore, instead of maximizing over all $\boldsymbol{\varphi}_i \in \Phi_i$, our theoretical investigation suggests that, for any given g , it suffices to define the profile likelihood function as $\ell_i^p(g | \mathcal{H}_T) = \ell_i(\widehat{\mathbf{w}}_g, \widehat{\boldsymbol{\theta}}_g, \widehat{\boldsymbol{\varphi}}_i^p(g) | \mathcal{H}_T)$, where

$$\widehat{\boldsymbol{\varphi}}_i^p(g) = \underset{\boldsymbol{\varphi}_i \in \{\widehat{\boldsymbol{\varphi}}_{g', \mathcal{G}_i} : g' \in [G], \mathcal{G}_i \in [G]^{d_i}\}}{\operatorname{argmax}} \ell_i(\widehat{\mathbf{w}}_g, \widehat{\boldsymbol{\theta}}_g, \boldsymbol{\varphi}_i | \mathcal{H}_T), \quad \text{for } g \in [G].$$

Denote $\widehat{g}_i^\dagger = \operatorname{argmax}_{1 \leq g \leq G} \ell_i^p(g | \mathcal{H}_T)$. The refined membership of node i (denoted as \widehat{g}_i^r) and the corresponding network effect parameter vector (denoted as $\widehat{\boldsymbol{\varphi}}_i^r$) are then defined as

$$\{\widehat{g}_i^r, \widehat{\boldsymbol{\varphi}}_i^r\} = \begin{cases} \{\widehat{g}_i, \widehat{\boldsymbol{\varphi}}_{\widehat{g}_i, \widehat{\mathcal{G}}_i}\}, & \text{if } \ell_i^p(\widehat{g}_i^\dagger | \mathcal{H}_T) - \ell_i(\widehat{\mathbf{w}}_{\widehat{g}_i}, \widehat{\boldsymbol{\theta}}_{\widehat{g}_i}, \widehat{\boldsymbol{\varphi}}_{\widehat{g}_i, \widehat{\mathcal{G}}_i} | \mathcal{H}_T) \leq \Delta_T^r, \\ \{\widehat{g}_i^\dagger, \widehat{\boldsymbol{\varphi}}_i^p(\widehat{g}_i^\dagger)\}, & \text{if } \ell_i^p(\widehat{g}_i^\dagger | \mathcal{H}_T) - \ell_i(\widehat{\mathbf{w}}_{\widehat{g}_i}, \widehat{\boldsymbol{\theta}}_{\widehat{g}_i}, \widehat{\boldsymbol{\varphi}}_{\widehat{g}_i, \widehat{\mathcal{G}}_i} | \mathcal{H}_T) > \Delta_T^r, \end{cases} \quad (17)$$

where Δ_T^r is a pre-chosen threshold sequence. After the refinement, we obtain the updated membership estimates $\mathcal{G}^r = (\widehat{g}_1^r, \widehat{g}_2^r, \dots, \widehat{g}_m^r)^\top$ and the transition matrix estimate $\widehat{\mathbf{B}}^r = (\widehat{b}_{ij}^r)$ with

$$\widehat{b}_{ij}^r = \widehat{\beta}_{\widehat{g}_i^r} I(i = j) + d_i^{-1} \widehat{\phi}_{ij}^r I(j \in \mathcal{N}_i), \quad i, j = 1, \dots, m, \quad (18)$$

where $\widehat{\phi}_{ij}^r$ equals $\sqrt{d_i}$ multiplies the element in $\widehat{\boldsymbol{\varphi}}_i^r$ corresponding to the node $j \in \mathcal{N}_i$, $i = 1, \dots, m$.

We remark that the membership refinement only occurs when a significant increment of the log-likelihood (more than Δ_T^r) can be achieved by switching memberships. Our theory requires $\Delta_T^r = o_p(1)$ as $T \rightarrow \infty$, which is trivially satisfied if we set $\Delta_T^r \equiv 0$. However, such a choice

may introduce too much additional variability in the refined membership estimates, especially when G is large, which may in turn result in inferior finite sample performance. In this work, we propose to use $\Delta_T^r = \frac{2}{G} \sum_{g=1}^G \widehat{\text{sd}}_g$, where $\widehat{\text{sd}}_g$ is the sample standard deviation of the set $\{\ell_i(\widehat{\mu}_{\widehat{g}_i}, \widehat{\boldsymbol{\theta}}_{\widehat{g}_i}, \widehat{\boldsymbol{\varphi}}_{\widehat{g}_i, \widehat{\mathcal{G}}_i}) : \widehat{g}_i = g, i = 1, \dots, m\}$, for $g \in [G]$. As demonstrated in Sections 5-6, this choice for Δ_T^r works well for our numerical examples.

3.5 Selection of Number of Groups

Denote the true number of latent groups as G_0 . Theorems 2-3 in Section 4 suggest that under suitable conditions the MLE of model parameters are consistent for their theoretical counterparts and all node memberships can be correctly estimated as long as $G \geq G_0$. However, according to Theorem 4, the asymptotic normality of $\widehat{\boldsymbol{\theta}}$ and $\widehat{\boldsymbol{\phi}}$ depends on the assumption that $G = G_0$. Therefore, it is of practical interest to develop a data-driven criterion to determine G_0 .

With a slight abuse of notation, we denote $\widehat{\mathbf{w}}^{(G)}, \widehat{\boldsymbol{\theta}}^{(G)}, \widehat{\boldsymbol{\phi}}^{(G)}, \widehat{\mathcal{G}}^{(G)}$ as the MLE obtained in (12) for a given G . We consider the following likelihood based criterion function,

$$\text{LIC}(G) = \ell(\widehat{\mathbf{w}}^{(G)}, \widehat{\boldsymbol{\theta}}^{(G)}, \widehat{\boldsymbol{\phi}}^{(G)}, \widehat{\mathcal{G}}^{(G)} | \mathcal{H}_T) - \lambda_{mT} G, \quad (19)$$

where $\ell(\cdot | \mathcal{H}_T)$ is as defined in (11) and $\lambda_{mT} > 0$ is a tuning parameter depending on m and T . The optimal G is selected by $\widehat{G} = \arg \max_G \text{LIC}(G)$. If λ_{mT} satisfies the condition (28), Theorem 5 shows that, under suitable conditions, one can select $\widehat{G} = G_0$ with probability tending to 1.

4 THEORETICAL PROPERTIES

We now investigate the asymptotic properties of the MLE (12). Denote $\mu_g^0(\cdot)$ as the true background intensity of group g and $\mu_g^*(\cdot) = \mathbf{w}_g^{*\top} \mathbf{x}_{n_{\text{kt}}}(\cdot)$ as the best spline approximation to $\mu_g^0(\cdot)$ with $\mathbf{w}_g^* = \arg \min_{\mathbf{w} \in \mathbb{W}} \|\mathbf{w}^\top \mathbf{x}_{n_{\text{kt}}}(\cdot) - \mu_g^0(\cdot)\|_\infty$, $g \in [G]$. By Assumption 2, one has that

$$\max_{1 \leq g \leq G} \|\mu_g^*(\cdot) - \mu_g^0(\cdot)\|_\infty = O(n_{\text{kt}}^{-r}). \quad (20)$$

Denote $\beta_g^0, \gamma_g^0, \phi_{gg'}^0$ as the true values of $\beta_g, \gamma_g, \phi_{gg'}$ respectively, for $g' \neq g, g, g' \in [G]$. Let $\mathcal{G}^0 = (g_1^0, \dots, g_m^0)^\top$ be the true membership vector, where $g_i^0 \in [G_0]$. Note that G and G_0 may be different in our theoretical framework. Correspondingly, $\underline{\theta}^0, \underline{\phi}^0, \underline{\mathcal{G}}^0$, and $\underline{\varphi}_{g_i^0, \mathcal{G}_i^0}^0, i = 1, \dots, m$, are defined by replacing parameters with the true values in their definitions.

4.1 Technical Assumptions

Denote $\underline{\psi} = (\underline{\mathbf{w}}^\top, \underline{\theta}^\top, \underline{\phi}^\top, \underline{\mathcal{G}}^\top)^\top$ and define the function $\bar{\ell}(\underline{\psi}) = \mathbb{E}[\ell(\underline{\psi}|\mathcal{H}_T)]$, which is of the form

$$\bar{\ell}(\underline{\psi}) = \frac{1}{m} \sum_{i=1}^m \bar{\ell}_i(\mathbf{w}_{g_i}, \theta_{g_i}, \varphi_{g_i, \mathcal{G}_i}), \text{ and } \bar{\ell}_i(\mathbf{w}_{g_i}, \theta_{g_i}, \varphi_{g_i, \mathcal{G}_i}) = \mathbb{E}[\ell_i(\mathbf{w}_{g_i}, \theta_{g_i}, \varphi_{g_i, \mathcal{G}_i}|\mathcal{H}_T)]. \quad (21)$$

To establish the parameter estimation consistency, we require the following assumptions.

Assumption 4. Define the parameter space $\Phi_i = \{\phi/\sqrt{d_i} : \phi \in \Phi\}^{d_i}$ and $\Omega_{i,\epsilon} = \{(\mathbf{w}, \theta, \varphi_i) \in \mathbb{W} \times \Theta \times \Phi_i : \|\mathbf{w} - \mathbf{w}_{g_i^0}^*\| + \|\theta - \theta_{g_i^0}^0\| + \|\varphi_i - \varphi_{g_i^0, \mathcal{G}_i^0}^0\| > \epsilon\}$. For any $\epsilon > 0$, there exist constants $C_1 > 0$ such that $\inf_{m \geq 1} \inf_{1 \leq i \leq m} \inf_{(\mathbf{w}, \theta, \varphi_i) \in \Omega_{i,\epsilon}} [\bar{\ell}_i(\mathbf{w}_{g_i^0}^*, \theta_{g_i^0}^0, \varphi_{g_i^0, \mathcal{G}_i^0}^0) - \bar{\ell}_i(\mathbf{w}, \theta, \varphi_i)] > \min\{C_1, \epsilon C(\epsilon)\}$, where $C(\epsilon)$ is a non-decreasing function of ϵ .

Assumption 5. The functions $\bar{\ell}_i(\mathbf{w}, \theta, \varphi_i)$'s are Lipschitz continuous in the sense that there exist a constant $M > 0$ such that $\sup_{1 \leq i \leq m} \sup_{\mathbf{w}, \mathbf{w}' \in \mathbb{W}, \theta, \theta' \in \Theta, \varphi_i, \varphi'_i \in \Phi_i} \frac{|\bar{\ell}_i(\mathbf{w}, \theta, \varphi_i) - \bar{\ell}_i(\mathbf{w}', \theta', \varphi'_i)|}{\|\mathbf{w} - \mathbf{w}'\| + \|\theta - \theta'\| + \|\varphi_i - \varphi'_i\|} \leq M$.

Assumption 6. There exists a $c_0 > 0$ such that $\inf_{g \neq g' \in [G_0]} [\|\mathbf{w}_g^* - \mathbf{w}_{g'}^*\| + \|\theta_g^0 - \theta_{g'}^0\|] > c_0$.

Assumption 7. Define $\pi_{g,m} = \frac{1}{m} \sum_{i=1}^m I(g_i^0 = g)$ and $\pi_{gg',m} = \frac{1}{m} \sum_{i=1}^m \sqrt{\frac{1}{d_i} \sum_{j \in \mathcal{N}_i} I(g_i^0 = g, g_j^0 = g')}$, $g, g' \in [G_0]$. Assume that as $m \rightarrow \infty$, $\pi_{g,m} \rightarrow \pi_g$ and $\pi_{gg',m} \rightarrow \pi_{gg'}$ and that there exists a constant $c_\pi > 0$ such that $\min_{g, g' \in [G_0]} \min\{\pi_g, \pi_{gg'}\} \geq c_\pi$.

Assumption 4 is a condition to ensure the identifiability of model parameters, which essentially requires that the expected log-likelihood functions, i.e., $\bar{\ell}_i(\mathbf{w}, \theta, \varphi_i)$'s, is locally maximized at the true parameters. This is a mild condition and similar conditions have been used in the literature, see, e.g., Liu et al. (2020). Assumption 5 imposes some smoothness condition on the expected node-wise log-likelihood, which is reasonable for the problem under consideration. Assumption 6

asserts that at least one of the background intensity or the node-specific parameter vector are well-separable between any two latent groups, which is a reasonable assumption for a wide range of applications such as the social network data studied in Section 6. Finally, Assumption 7 requires that there is a sufficient number of nodes in each latent group and that there is a sufficient number of connected nodes between any two different latent groups.

4.2 Model Estimation Consistency

Define the pseudo distance between $\underline{\psi} = (\underline{\mathbf{w}}^\top, \underline{\boldsymbol{\theta}}^\top, \underline{\boldsymbol{\phi}}^\top, \underline{\mathcal{G}}^\top)^\top \in \mathbb{W}^G \times \boldsymbol{\Theta}^G \times \boldsymbol{\Phi}^{G^2} \times \mathbb{G}$ and $\underline{\psi}' = (\underline{\mathbf{w}}'^\top, \underline{\boldsymbol{\theta}}'^\top, \underline{\boldsymbol{\phi}}'^\top, \underline{\mathcal{G}}'^\top) \in \mathbb{W}^{G'} \times \boldsymbol{\Theta}^{G'} \times \boldsymbol{\Phi}^{G'^2} \times \mathbb{G}$ as

$$d_m(\underline{\psi}', \underline{\psi}) = \frac{1}{m} \sum_{i=1}^m \left[\left\| \mathbf{w}'_{g'_i} - \mathbf{w}_{g_i} \right\| + \left\| \boldsymbol{\theta}'_{g'_i} - \boldsymbol{\theta}_{g_i} \right\| + \left\| \boldsymbol{\varphi}'_{g'_i, \mathcal{G}'_i} - \boldsymbol{\varphi}_{g_i, \mathcal{G}_i} \right\| \right], \quad (22)$$

where G and G' may be different. The following theorem states the parameter estimation consistency of the MLE (12) when the number of latent groups, i.e., G , is potentially over-specified.

Theorem 2. Define $\tau_m = \left\| \mathbf{1}^\top [\mathbf{I} - (1 + \delta)B]^{-1} \right\|_\infty$, where $\delta = (c_B^{-1} - 1)/2$ with c_B defined in Assumption 1. Under Assumptions 1–7 and assume that $G \geq G_0$ and that as $m \rightarrow \infty, T \rightarrow \infty$,

$$T^{-1}(\log mT)^{7+} \tau_m^{5+} b^{3+} \max\{n_{\text{kt}}, \tau_m^2 b^2 [\log(mT)]^4\} = O(1), \quad (23)$$

where $z+$ stands for any number greater than z . Then it holds that as $m, T \rightarrow \infty$,

- (a). $d_m(\underline{\hat{\psi}}, \underline{\psi}^*) = o_p(1)$ where $\underline{\hat{\psi}}$ is defined in (12) and $\underline{\psi}^* = (\underline{\mathbf{w}}^{*\top}, \underline{\boldsymbol{\theta}}^{0\top}, \underline{\boldsymbol{\phi}}^{0\top}, \underline{\mathcal{G}}^{0\top})^\top$;
- (b). $\sup_{1 \leq i \leq m} \left[\left\| \hat{\mu}_{\hat{g}_i^r}(\cdot) - \mu_{g_i^0}^0(\cdot) \right\|_T + \left\| \hat{\boldsymbol{\theta}}_{\hat{g}_i^r} - \boldsymbol{\theta}_{g_i^0}^0 \right\| \right] = o_p(1)$ where \hat{g}_i^r is the estimated membership of node i after refinement, $i = 1, \dots, m$, and $\hat{\mu}_g(\cdot) = \hat{\mathbf{w}}_g^\top \mathbf{x}_{n_{\text{kt}}}(\cdot)$ for $g \in [G]$;
- (c). $\left\| \hat{\mathbf{B}}^r - \mathbf{B}^0 \right\|_\infty = o_p(1)$, where $\hat{\mathbf{B}}^r$ is given in (18) and \mathbf{B}^0 is the true \mathbf{B} in Assumption 1.

The proof is given in the Supplementary Material.

Theorem 2 asserts that even if G is over-specified, all model parameters can still be consistently estimated. In particular, the background intensity $\mu_{g_i}^0(\cdot)$ and the node-specific parameters

$\theta_{g_i^0}^0$ can still be consistently estimated for all network nodes. Furthermore, the transition matrix \mathbf{B}^0 that involves all $\phi_{g_i g_j}^0$'s can also be consistently estimated, which is of important practical interest since the estimated $\hat{\mathbf{B}}^r$ can be used to study the network interactions following Section 2.3. However, we remark that Theorem 2 is unlikely to hold when $G < G_0$, in which case nodes from different groups are forced into the same group, resulting in biased parameter estimators.

Some remarks are in order for condition (23). As the range of triggering function's, i.e., b , increases, the dependence becomes stronger among observed event times and renders the need for a larger T . Furthermore, by Theorem 1, τ_m is roughly (when $\delta = 0$) the average number of offspring events on the network that are triggered by a parent event occurring on the most influential node. In this sense, τ_m can be viewed as a measure of the network connectivity level. A larger τ_m would potentially result in more clustered event times and it would require a larger T to offset such an effect for model estimation. Condition (23) requires that τ_m cannot exceed the order of $O(T^{1/8})$ as m increases, which is an upper bound new to the literature.

Next, we discuss the membership estimation consistency when $G \geq G_0$. For each $g \in [G]$, define $\hat{\mathcal{C}}_g = \{i : 1 \leq i \leq m, \text{ and } \hat{g}_i^r = g\}$ and for any $g' \in [G_0]$, define $\mathcal{C}_{g'}^0 = \{i : 1 \leq i \leq m, \text{ and } g_i^0 = g'\}$. The next theorem establishes the group membership estimation consistency.

Theorem 3. *Suppose $G \geq G_0$ and assume Assumptions 1–7 and (23) hold. Then for each $g \in [G]$, there exists a $g' \in [G_0]$ such that $P(\hat{\mathcal{C}}_g \subset \mathcal{C}_{g'}^0) \rightarrow 1$ as $m, T \rightarrow \infty$.*

The proof is given in the Supplementary Material.

Theorem 3 states that group memberships of all nodes can be consistently estimated when $G \geq G_0$, which is stronger than the existing membership estimation consistency results in the community detection literature (Zhao et al., 2012). When $G = G_0$, Theorem 3 asserts that after some label permutation, one has that $\hat{\mathcal{C}}_g = \mathcal{C}_g^0$ for any $g \in [G_0]$ with a probability tending to 1.

4.3 Convergence Rates and Asymptotic Normality

We now study the convergence rates of the background intensity estimators and the asymptotic normality of the model parameter estimators when $G = G_0$. Define the “oracle” estimator $(\hat{\mathbf{w}}^{\text{or}\top}, \hat{\boldsymbol{\theta}}^{\text{or}\top}, \hat{\boldsymbol{\phi}}^{\text{or}\top})^\top = \arg\max_{\mathbf{w}, \boldsymbol{\theta}, \boldsymbol{\phi}} \ell(\mathbf{w}, \boldsymbol{\theta}, \boldsymbol{\phi}, \mathcal{G}^0 | \mathcal{H}_T)$, where the true group membership \mathcal{G}^0 is known. Denote the refitted estimator $(\hat{\mathbf{w}}^{r\top}, \hat{\boldsymbol{\theta}}^{r\top}, \hat{\boldsymbol{\phi}}^{r\top})^\top = \arg\max_{\mathbf{w}, \boldsymbol{\theta}, \boldsymbol{\phi}} \ell(\mathbf{w}, \boldsymbol{\theta}, \boldsymbol{\phi}, \hat{\mathcal{G}}^r | \mathcal{H}_T)$ with $\hat{\mathcal{G}}^r$ being the refined membership estimator. The following Proposition states that when $G = G_0$, the aforementioned two parameter estimators are asymptotically equivalent.

Proposition 1. *Suppose $G = G_0$ and assume Assumptions 1-7 and equation (23) hold. Then it holds that $P\left(\{\hat{\mathbf{w}}^r = \hat{\mathbf{w}}^{\text{or}}\} \cap \{\hat{\boldsymbol{\theta}}^r = \hat{\boldsymbol{\theta}}^{\text{or}}\} \cap \{\hat{\boldsymbol{\phi}}^r = \hat{\boldsymbol{\phi}}^{\text{or}}\}\right) \rightarrow 1$ as $m, T \rightarrow \infty$.*

The proof is given in the Supplementary Material.

Proposition 1 suggests that when $G = G_0$, to study the distributional properties of the refitted estimator, it suffices to derive the asymptotic distribution of the “Oracle” estimator by fixing $\mathcal{G} = \mathcal{G}_0$. For ease of presentation, in what follows, we drop the notation \mathcal{G}_0 whenever there is no ambiguity. In particular, the model parameters need to be estimated becomes $\underline{\boldsymbol{\psi}} = (\underline{\mathbf{w}}^\top, \underline{\boldsymbol{\theta}}^\top, \underline{\boldsymbol{\phi}}^\top)^\top$, whose true values are $\underline{\boldsymbol{\psi}}^* = (\underline{\mathbf{w}}^{*\top}, \underline{\boldsymbol{\theta}}^{0\top}, \underline{\boldsymbol{\phi}}^{0\top})^\top$.

For any given $\underline{\boldsymbol{\psi}}$, we view the conditional intensity function (10) as a function of $\underline{\boldsymbol{\psi}}$ and denote it as $\lambda_i(t|\underline{\boldsymbol{\psi}}, \mathcal{H}_t)$ for any $t \in [0, T]$ and $i = 1, \dots, m$. Define the matrix

$$\mathbf{H}_{mT}(\underline{\boldsymbol{\psi}}) = \frac{1}{mT} \sum_{i=1}^m \int_0^T \mathbb{E} \left[\lambda_i^0(t|\mathcal{H}_t) \frac{\dot{\lambda}_i(t|\underline{\boldsymbol{\psi}}, \mathcal{H}_t)}{\lambda_i(t|\underline{\boldsymbol{\psi}}, \mathcal{H}_t)} \frac{\dot{\lambda}_i^\top(t|\underline{\boldsymbol{\psi}}, \mathcal{H}_t)}{\lambda_i(t|\underline{\boldsymbol{\psi}}, \mathcal{H}_t)} \right] dt, \quad (24)$$

where $\lambda_i^0(\cdot|\mathcal{H}_t)$ is the true conditional intensity and $\dot{\lambda}_i(\cdot|\underline{\boldsymbol{\psi}}, \mathcal{H}_t) = \partial \lambda_i(\cdot|\underline{\boldsymbol{\psi}}, \mathcal{H}_t) / \partial \underline{\boldsymbol{\psi}}$, $i = 1, \dots, m$.

Assumption 8. *There exist positive constants $\epsilon, \tau_{\min}, \tau_{\max}$ such that for any $\|\underline{\boldsymbol{\psi}} - \underline{\boldsymbol{\psi}}^*\| \leq \epsilon$, one has that $\lambda_{\min}[\mathbf{H}_{mT}(\underline{\boldsymbol{\psi}})] \geq \tau_{\min}$ and $\lambda_{\max}[\mathbf{H}_{mT}(\underline{\boldsymbol{\psi}})] \leq \tau_{\max}$ for sufficiently large m, T .*

Lemma ?? in the Supplementary Material shows that, under suitable conditions, $\mathbf{H}_{mT}(\underline{\boldsymbol{\psi}})$ is asymptotically equivalent to the negative Hessian matrix of expected log-likelihood $\bar{\ell}(\underline{\boldsymbol{\psi}})$ (when

$\mathcal{G} = \mathcal{G}^0$) in (21). Therefore, Assumption 8 essentially assumes that $\bar{\ell}(\underline{\psi})$ is locally convex in a neighborhood of $\underline{\psi}^*$, which is a mild assumption similar to Assumption 4.

The following theorem establishes the convergence rates of the background intensity estimators and the asymptotic normality of the model parameters.

Theorem 4. *Under Assumptions 1-8 and assume (23) hold. If $G = G_0$, it holds that*

(a). *Let $n_{\text{kt},b} = \max\{n_{\text{kt}}, \tau_m^2 b^2 [\log(mT)]^4\}$ and assume that*

$$\frac{(\tau_m b)^3 [\log(mT)]^3 n_{\text{kt}} (n_{\text{kt},b})^2 \log(n_{\text{kt},b})}{T} = o(1) \text{ and } \frac{n_{\text{kt},b} \tau_m b [\log(mT)]^2}{n_{\text{kt}}^r} = o(1). \quad (25)$$

Then as $m, T \rightarrow \infty$, one has that

$$\max_{1 \leq g \leq G} \|\hat{\mu}_g(\cdot) - \mu_g^0(\cdot)\|_T = O_p \left[(mT)^{-1/2} \sqrt{n_{\text{kt},b} \tau_m b \log(mT)} + n_{\text{kt}}^{-r} \sqrt{n_{\text{kt},b}} \right]. \quad (26)$$

(b). *Denote $\hat{\underline{\alpha}} = (\hat{\underline{\theta}}^\top, \hat{\underline{\phi}}^\top)^\top$, $\underline{\alpha}^0 = (\underline{\theta}^{0\top}, \underline{\phi}^{0\top})^\top$, and let $\underline{\Sigma}_\alpha = \lim_{(m,T) \rightarrow \infty} \mathcal{I}_\alpha \mathbf{H}_{mT}^{-1}(\underline{\psi}^*) \mathcal{I}_\alpha^\top$ with*

$\mathcal{I}_\alpha = (\mathbf{0}_{(3G+G^2) \times n_{\text{kt}}}, \mathbf{I}_{(3G+G^2) \times (3G+G^2)})$. If it holds that $r > 2$ and that

$$\frac{(mT)^{1/2}}{n_{\text{kt}}^r \sqrt{\tau_m b \log(mT)}} = o(1), \text{ and } \frac{n_{\text{kt},b}^4 \tau_m^3 b^3 [\log(mT)]^4}{mT} = o(1), \quad (27)$$

then one has that $\sqrt{mT}(\hat{\underline{\alpha}} - \underline{\alpha}^0) \xrightarrow{d} N(\mathbf{0}, \underline{\Sigma}_\alpha)$ as $m, T \rightarrow \infty$.

The proof is given in the Supplementary Material.

Theorem 4 part (a) gives an upper bound of the convergence rate of nonparametric background intensity estimators, although (26) may not be the sharp upper bound. The convergence rate in (26) slows down when b and τ_m increase, which is reasonable because larger b and τ_m indicate a greater level of dependence among observed event times on the network. Part (b) gives sufficient conditions under which the \sqrt{mT} -convergence rate for $\underline{\alpha}^0$ and the asymptotic normality can be established. The result is proved by using a martingale Central Limit Theorem (Fleming and Harrington, 2011). An unbiased estimator of the covariance matrix $\underline{\Sigma}_\alpha$ can be constructed straightforwardly using the definition of $\mathbf{H}_{mT}(\underline{\psi}^*)$ in (24) for valid statistical inferences.

4.4 Selection Consistency of Number of Groups

In this subsection, we study the selection consistency of the LIC criterion proposed in (19). To this end, we show in the following Theorem that \hat{G} selected by maximizing LIC estimates G_0 consistently when the penalty parameter λ_{mT} is appropriately chosen.

Theorem 5. *Assume Assumptions 1-7, (23), and (25). Let $\bar{d} = \frac{1}{m} \sum_{i=1}^m d_i$, and assume that*

$$\lambda_{mT} \rightarrow 0, \text{ and } \lambda_{mT}^{-1} \left([\log(mT)]^2 \tau_m^2 b \sqrt{T^{-1} \bar{d} [n_{\text{kt},b} \log(n_{\text{kt}} \bar{d}) + \log(m)]} \right) \rightarrow 0, \quad (28)$$

where $n_{\text{kt},b} = \max\{n_{\text{kt}}, \tau_m^2 b^2 [\log(mT)]^4\}$. We have that $P(\hat{G} = G_0) \rightarrow 1$ as $m, T \rightarrow \infty$.

The proof is given in the Supplementary Material.

Condition (28) requires that λ_{mT} converges to zero but not too fast. In our numerical examples, we set $\lambda_{mT} = (15T)^{-1} (\text{median}_{1 \leq i \leq m} n_i)^{0.6} \bar{d}^{0.25}$ and verify its finite sample performances in details in Section 5. Such a choice ensures that \hat{G} does not depend on the unit of T .

5 Simulation Studies

In this section, we conduct simulation studies to evaluate the numerical performance of the proposed GNHP model. The following two types of network structures are considered:

STOCHASTIC BLOCK MODEL (SBM). This model is widely used in the community detection literature (Wang and Wong, 1987; Karrer and Newman, 2011). The network consists of m nodes belonging to 3 blocks and each node is randomly assigned a block label with a probability of $1/3$. An edge between two nodes is generated with a probability $0.3m^{-0.3}$ if they are in the same block, or with a probability of $0.3m^{-0.8}$ otherwise.

POWER-LAW NETWORK. This type of network resembles the commonly observed social network structure where most nodes have few followers while a small fraction of nodes have a large number of followers. For each node i , the number of randomly picked followers f_i follows the power-law distribution $P(f_i = f) = cf^{-2}, 0 \leq f \leq m$, where c is the normalizing constant.

For each type of network, we random assign each node to $G_0 = 3$ latent groups with group proportions as $\boldsymbol{\pi}_m = (\pi_{1,m}, \pi_{2,m}, \pi_{3,m})^\top = (0.3, 0.4, 0.3)^\top$. To mimic typical daily activities of social network users, the background intensity of each latent group takes a periodic form

$$\mu_g(t) = \nu_{0,g} + \nu_{1,g} \sum_{h=1}^{H_g} \sin\left(\frac{t - a_{h,g}}{\omega_0} \pi\right) \mathbf{1}\{a_{h,g} \leq t \leq a_{h,g} + \omega_0\}, \quad g \in [G_0].$$

The triggering functions for all latent groups are specified as $f(t, \gamma) \propto \gamma \exp(-\gamma t) \mathbf{1}\{t \leq b\}$ with $b = 5$ hours. Model parameters are listed in Table 1 and the resulting background intensities are illustrated in Figure 3. The common period for $\mu_g(\cdot)$'s is set as $\omega = 12$ hours and the parameter $\nu_{0,g}$ is chosen such that $\int_0^\omega \mu_g(t) dt$ is set at the targeted values in Table 1.

g	Background intensity						Momentum		Network	
	H_g	$\nu_{1,g}/\nu_{0,g}$	$a_{1,g}$	$a_{2,g}$	ω_0	$\int_0^\omega \mu_g(t) dt$	β_g	η_g	γ_g	$(\phi_{g1}, \phi_{g2}, \phi_{g3})$
1	1	4	3	-	1	1.5	0.5	1.5	1	(0.4, 0.1, 0.1)
2	1	6	7	-	2	1	0.4	1	2	(0.6, 0.4, 0.5)
3	2	2	5	8	1	0.5	0.7	2	0.5	(0.15, 0.2, 0.1)

Table 1: Parameter setting for $G_0 = 3$ groups.

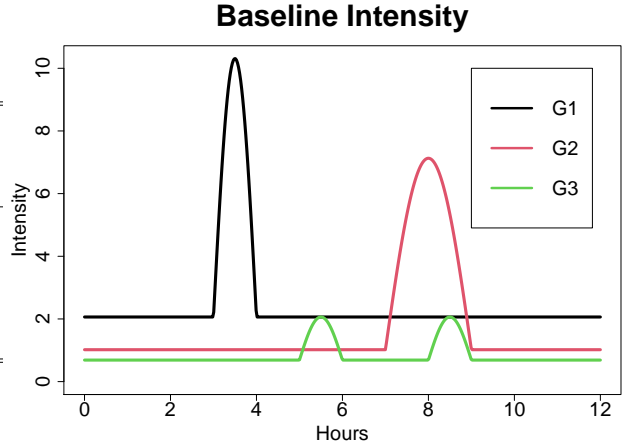


Figure 3: True background intensities.

Data are simulated from model (2) with $m \in \{100, 200\}$ and $T \in \{5\omega, 10\omega, 20\omega, 40\omega\}$. B-splines are used to approximate the background intensity $\mu_g(\cdot)$'s, with $n_{\text{kt}} = 36$ equally spaced internal knots between $[0, \omega]$. For each (m, T) , summary statistics are computed based on $K = 500$ simulation runs. For the k th simulation run, we denote the estimators as $\{\hat{\mu}_g^{(k)}(\cdot), \hat{\beta}_g^{(k)}, \hat{\eta}_g^{(k)}, \hat{\gamma}_g^{(k)}, \hat{\phi}_{gg'}^{(k)}\}$ and the refined group membership estimator as $\{\hat{g}_i^{r(k)} : 1 \leq i \leq m\}$.

5.1 Estimation Accuracy When $G = G_0$

When $G = G_0$, parameter estimation accuracy can be directly evaluated by the root mean squared error (RMSE) of the parameter estimates after some label switching. The estimation ac-

curacy of the background intensity $\mu_g(\cdot)$ is evaluated by $K^{-1} \sum_{k=1}^K \int |\hat{\mu}_g^{(k)}(t) - \mu_g(t)| dt$. The group membership estimation accuracy rate is computed by $\text{GAR} = K^{-1} \sum_{k=1}^K \{m^{-1} \sum_{i=1}^m I(\hat{g}_i^{r(k)} = g_i^0)\}$. As a comparison baseline, we also present estimation accuracy of the “Oracle” estimator for which the true group membership of all nodes are known and fixed when finding the MLE. All simulation results are summarized in Tables 2-3.

Table 2: Estimation Accuracy of GNHP for SBM network when $G = G_0$.

$m = 100$									
T	$\mu \ (\times 10^{-3})$	$\beta (\times 10^{-3})$	$\eta \ (\times 10^{-3})$	$\gamma \ (\times 10^{-3})$	$\phi \ (\times 10^{-3})$			GAR	
	GNHP (Oracle)	GNHP (Oracle)	GNHP (Oracle)	GNHP (Oracle)	GNHP (Oracle)				
g/g'	-	-	-	-	1	2	3		
5ω	1	311 (268)	18.2 (15.2)	66.7 (58.6)	75.8 (62.6)	31.9 (23.8)	24.0 (14.2)	32.2 (17.4)	0.900
	2	268 (229)	21.4 (16.1)	61.1 (49.0)	136.2 (114.3)	39.5 (33.5)	37.0 (35.3)	57.5 (42.4)	
	3	234 (166)	32.2 (25.2)	107.3 (96.8)	51.0 (42.2)	25.6 (18.5)	28.7 (22.8)	37.3 (23.4)	
10ω	1	216 (202)	11.7 (11.3)	45.5 (45.2)	44.2 (43.8)	26.6 (18.6)	13.0 (10.2)	14.2 (10.6)	0.981
	2	184 (167)	19.3 (12.8)	57.3 (35.9)	105.2 (77.1)	32.2 (23.9)	33.6 (24.4)	35.0 (31.9)	
	3	143 (119)	22.8 (17.7)	82.9 (70.5)	72.4 (26.2)	22.8 (11.5)	22.7 (16.9)	22.3 (14.1)	
20ω	1	163 (159)	8.3 (7.8)	28.3 (28.2)	30.5 (30.5)	13.1 (12.1)	7.7 (7.1)	8.5 (8.1)	0.993
	2	135 (129)	9.8 (9.5)	25.6 (23.3)	59.4 (51.9)	18.7 (17.6)	17.5 (18.1)	23.2 (22.1)	
	3	101 (93)	12.2 (12.0)	49.2 (48.0)	19.6 (19.2)	9.0 (9.6)	12.2 (11.4)	13.0 (10.9)	
40ω	1	134 (131)	5.8 (5.7)	22.6 (22.7)	21.1 (19.2)	8.4 (7.8)	5.3 (4.9)	6.7 (6.4)	0.994
	2	109 (107)	6.4 (6.3)	17.2 (17.0)	37.7 (37.5)	12.4 (12.0)	13.1 (12.8)	14.6 (14.6)	
	3	87 (78)	9.0 (8.9)	35.2 (35.0)	14.4 (13.6)	6.4 (6.4)	8.3 (8.3)	10.7 (7.6)	
$m = 200$									
5ω	1	211 (201)	11.1 (10.4)	40.8 (37.7)	41.6 (41.0)	17.3 (17.3)	9.6 (8.6)	11.5 (10.9)	0.977
	2	195 (168)	12.5 (12.4)	34.8 (33.6)	72.6 (71.0)	25.0 (23.9)	22.7 (22.8)	29.9 (28.8)	
	3	130 (120)	18.2 (17.2)	67.0 (63.6)	28.9 (28.1)	12.5 (11.1)	15.6 (15.3)	13.7 (13.3)	
10ω	1	160 (156)	8.2 (7.8)	29.0 (27.4)	31.4 (31.1)	11.7 (11.6)	6.9 (6.8)	7.5 (7.3)	0.994
	2	141 (131)	8.4 (8.4)	21.9 (21.5)	50.4 (49.8)	16.5 (16.4)	15.4 (15.4)	19.6 (19.6)	
	3	97 (92)	11.6 (11.6)	42.2 (42.6)	18.7 (18.7)	8.6 (8.6)	10.4 (10.3)	9.6 (9.5)	
20ω	1	141 (130)	5.8 (5.8)	20.3 (20.2)	22.4 (22.1)	8.6 (7.8)	4.9 (4.8)	5.4 (5.3)	0.995
	2	126 (113)	6.1 (6.0)	15.7 (15.3)	32.3 (32.7)	11.9 (11.8)	11.4 (10.6)	15.4 (15.4)	
	3	83 (76)	8.7 (8.7)	34.0 (33.9)	14.1 (14.1)	5.9 (5.5)	7.2 (7.2)	6.6 (6.6)	
40ω	1	130 (112)	3.8 (3.8)	15.4 (15.2)	17.2 (17.2)	6.1 (5.7)	3.3 (3.3)	3.8 (3.8)	0.998
	2	98 (98)	4.1 (4.1)	11.8 (11.7)	25.0 (25.4)	8.2 (8.2)	8.2 (8.1)	9.8 (9.9)	
	3	70 (68)	6.1 (6.1)	22.6 (22.6)	9.5 (9.5)	4.0 (4.1)	5.1 (5.2)	4.7 (4.6)	

From Tables 2-3, we can see that when both m and T are small, the group memberships of a large proportion of network nodes may be incorrectly estimated in both network settings. As m and/or T increases, the GAR gradually approaches 1. This is consistent with our theoretical findings in Theorem 3. Consequently, as m or T increases, the estimation accuracy of the model parameters improves steadily and approaching that of the “Oracle” estimator. Overall, the simulation results support the estimation consistency of the proposed GNHP model when the

Table 3: Estimation Accuracy of GNHP for Power Law network when $G = G_0$.

RMSE TABLE, PL setting.									
$m = 100$									
T	$\mu (\times 10^{-3})$	$\beta (\times 10^{-3})$	$\eta (\times 10^{-3})$	$\gamma (\times 10^{-3})$	$\phi (\times 10^{-3})$			GAR	
	GNHP (Oracle)	GNHP (Oracle)	GNHP (Oracle)	GNHP (Oracle)	GNHP (Oracle)				
g/g'	-	-	-	-	1	2	3		
5ω	1	320 (268)	18.9 (15.1)	61.1 (56.3)	98.4 (77.8)	76.4 (33.2)	53.9 (21.6)	69.8 (23.1)	0.886
	2	279 (231)	23.7 (17.8)	66.9 (51.2)	168.1 (129.8)	85.3 (46.6)	88.2 (52.5)	120.3 (71.4)	
	3	262 (168)	35.9 (25.5)	115.1 (107.4)	61.8 (43.1)	35.2 (25.6)	43.9 (31.6)	50.0 (32.9)	
10ω	1	218 (203)	12.9 (11.1)	43.9 (43.2)	57.4 (50.4)	46.8 (28.2)	27.7 (15.1)	34.9 (15.8)	0.972
	2	187 (167)	16.3 (13.6)	45.1 (36.4)	102.0 (89.8)	63.6 (37.0)	57.8 (54.8)	107.7 (42.7)	
	3	143 (120)	19.3 (18.0)	71.1 (70.5)	31.8 (30.3)	20.0 (17.6)	27.9 (23.1)	26.9 (19.8)	
20ω	1	162 (161)	9.6 (8.5)	32.3 (28.3)	40.3 (39.8)	24.4 (16.3)	11.9 (9.9)	15.2 (11.3)	0.996
	2	130 (129)	12.3 (10.2)	34.3 (26.2)	77.1 (68.3)	51.9 (24.4)	34.9 (34.0)	73.7 (28.6)	
	3	99 (93)	14.4 (14.3)	53.3 (49.7)	29.6 (23.2)	14.8 (13.6)	20.5 (17.2)	19.9 (16.6)	
40ω	1	135 (131)	6.3 (6.2)	20.9 (20.4)	28.8 (26.4)	30.5 (14.1)	17.1 (6.6)	24.6 (7.5)	0.998
	2	118 (107)	7.2 (6.6)	19.3 (18.5)	49.9 (48.4)	33.5 (18.6)	27.1 (17.5)	38.7 (22.8)	
	3	80 (78)	9.9 (9.6)	35.2 (33.5)	17.7 (16.8)	8.8 (8.1)	12.3 (12.0)	11.5 (9.1)	
$m = 200$									
5ω	1	219 (205)	12.5 (12.1)	42.1 (40.2)	51.1 (47.7)	33.8 (20.9)	19.9 (12.2)	36.6 (13.0)	0.963
	2	175 (163)	13.0 (12.0)	35.9 (33.4)	82.0 (78.1)	33.3 (33.3)	28.9 (28.0)	49.4 (38.8)	
	3	146 (119)	20.7 (18.0)	71.6 (62.5)	35.2 (33.4)	16.3 (14.9)	22.9 (18.1)	22.9 (17.3)	
10ω	1	164 (160)	8.1 (7.7)	30.2 (29.7)	35.7 (33.0)	19.0 (14.6)	9.4 (8.9)	13.9 (9.6)	0.993
	2	136 (127)	8.9 (8.9)	24.3 (24.3)	59.4 (58.7)	21.4 (21.0)	21.1 (19.3)	40.2 (23.5)	
	3	102 (93)	12.1 (12.1)	47.7 (47.3)	21.1 (20.6)	9.8 (8.6)	14.5 (14.2)	13.4 (12.2)	
20ω	1	134 (131)	6.4 (5.9)	20.8 (19.9)	26.1 (27.1)	16.8 (10.3)	6.1 (5.8)	8.2 (6.6)	0.998
	2	111 (107)	6.8 (6.9)	17.0 (16.9)	43.2 (42.9)	16.1 (14.7)	14.4 (14.3)	28.6 (17.3)	
	3	78 (78)	9.0 (8.7)	33.1 (31.6)	15.0 (14.3)	7.5 (7.7)	9.6 (8.3)	8.5 (7.5)	
40ω	1	113 (113)	4.2 (4.2)	14.7 (14.9)	18.2 (18.1)	13.7 (7.8)	12.1 (4.3)	4.5 (4.3)	0.999
	2	95 (93)	4.4 (4.3)	12.6 (12.9)	29.9 (29.7)	13.6 (10.8)	12.3 (10.9)	11.9 (11.9)	
	3	69 (69)	6.5 (6.3)	23.7 (21.9)	10.9 (10.9)	5.2 (4.8)	7.7 (7.3)	5.5 (5.6)	

group number G is correctly specified.

5.2 Coverage Probability When $G = G_0$

We next investigate the quality of statistical inference for the GNHP model by evaluating the coverage probabilities of the 95% confidence intervals for model parameters, derived through the limiting distribution given by Theorem 4 (b). For instance, the 95% confidence interval for β_g is given by $\text{CI}_{\beta_g}^{(k)} = (\hat{\beta}_g^{(k)} - 1.96\hat{\sigma}_{\beta_g}^{(k)}, \hat{\beta}_g^{(k)} + 1.96\hat{\sigma}_{\beta_g}^{(k)})$, where $\hat{\sigma}_{\beta_g}^{(k)}$ is the square root of the corresponding diagonal entry of the estimated covariance matrix Σ_α . Empirical coverage probabilities based on 500 simulation runs are summarized in Table 4.

Table 4 shows that the coverage probabilities have some departure from the nominal 95%

Table 4: Empirical coverage probabilities (%) for the GNHP model parameters.

		SBM network												Power Law network											
		$m = 100$						$m = 200$						$m = 100$						$m = 200$					
T	g/g'	β_g	η_g	γ_g	$\phi_{gg'}$			β_g	η_g	γ_g	$\phi_{gg'}$			β_g	η_g	γ_g	$\phi_{gg'}$			β_g	η_g	γ_g	$\phi_{gg'}$		
		-	-	-	1	2	3	-	-	-	1	2	3	-	-	-	1	2	3	-	-	-	1	2	3
5ω	1	85.2	87.0	83.6	85.6	81.4	85.6	93.2	94.2	93.4	92.8	92.4	93.0	83.8	83.2	79.0	76.2	75.8	73.0	91.6	91.6	92.2	90.2	91.0	88.4
	2	83.4	81.4	82.2	85.6	87.6	81.4	93.8	90.8	95.0	92.8	94.0	93.2	82.2	79.8	81.2	80.4	80.8	77.2	92.8	92.0	93.8	92.0	94.6	90.0
	3	81.6	85.2	81.2	83.2	83.6	77.6	93.2	93.2	94.4	93.0	93.2	92.8	77.2	81.8	81.2	79.0	80.0	70.0	89.6	91.2	91.6	91.8	91.0	88.0
10ω	1	92.0	91.8	93.8	92.2	90.0	94.6	94.0	95.0	93.8	94.2	94.2	94.6	93.0	92.0	93.0	88.8	90.0	88.6	93.6	92.8	94.6	95.4	92.0	93.4
	2	91.6	93.0	93.4	94.2	93.0	93.0	94.2	96.0	93.8	95.2	96.0	94.2	88.6	88.8	89.6	92.0	87.0	82.0	93.8	94.4	94.8	93.6	94.2	94.4
	3	92.2	92.2	92.8	95.2	91.8	92.2	96.0	95.0	95.2	93.6	96.0	94.6	92.4	91.6	92.2	90.6	88.8	86.4	93.6	95.0	95.0	94.6	93.6	92.4
20ω	1	95.0	97.4	94.4	93.4	93.6	95.0	94.6	95.0	94.8	94.0	93.2	94.0	93.0	92.2	93.2	93.6	92.8	92.4	93.6	94.4	94.4	96.0	94.0	95.2
	2	92.2	93.4	92.8	93.6	94.0	92.8	92.8	94.2	97.2	94.6	94.2	92.8	93.2	93.4	95.0	91.2	94.4	92.4	93.0	95.8	93.4	94.0	95.2	95.6
	3	94.8	94.4	96.0	95.2	94.4	94.4	93.8	93.4	92.8	94.0	95.4	94.0	93.8	95.0	93.0	91.8	94.2	93.2	94.8	96.0	95.4	95.6	93.2	93.8
40ω	1	93.8	95.0	95.6	94.4	93.0	92.6	96.2	94.0	92.0	94.0	94.8	95.4	93.0	95.0	93.6	92.6	94.0	95.0	94.6	95.2	95.2	95.2	94.4	96.8
	2	93.8	93.6	95.6	94.0	94.6	93.2	96.2	93.8	93.6	95.8	94.0	95.6	93.2	93.0	94.0	92.4	91.4	93.6	95.4	93.8	94.8	94.0	94.6	97.0
	3	93.4	93.4	94.8	93.8	94.4	92.8	93.6	95.6	94.0	95.2	96.2	94.4	92.6	93.4	94.0	93.0	93.0	93.2	95.0	94.6	94.8	95.2	95.2	96.0

when $m = 100$ and $T = 5\omega$ in both network settings, which is not surprising since on average only around 10% and 11% of group memberships are correctly estimated in these two settings. As m and T increase, the empirical coverage probabilities for almost all parameters approach the nominal level, which supports our theoretical findings in Theorem 4.

5.3 Estimation Accuracy with a Mis-specified G

When G is mis-specified, we evaluate the estimation accuracy by measures similar to the pseudo distance (22). For instance, we define $\text{PD}_\beta = \text{median}_{1 \leq k \leq K} \left\{ \frac{1}{m} \sum_{i=1}^m |\beta_{g_i^0}^0 - \hat{\beta}_{\hat{g}_i^{(k)}}^{(k)}| \right\}$, and PD_η and PD_γ are similarly defined. For the estimated background intensities, the pseudo distance is defined as $\text{PD}_\mu = \text{median}_{1 \leq k \leq K} \left\{ \frac{1}{m} \sum_{i=1}^m \int |\hat{\mu}_{\hat{g}_i^{(k)}}(t) - \mu_{g_i^0}^0(t)| dt \right\}$, and for the network effects, we evaluate the estimation accuracy of the transition matrix \mathbf{B} using $\text{PD}_\mathbf{B} = \text{median}_{1 \leq k \leq K} \left\{ \sqrt{\frac{1}{m} \sum_{i=1}^m \sum_{j=1}^m a_{ij} |\hat{b}_{ij}^{(k)} - b_{ij}^0|^2} \right\}$. To identify the true number of groups, the LIC in (19) is applied with $\lambda_{mT} = (15T)^{-1} (\text{median}_{1 \leq i \leq m} n_i)^{0.6} \bar{d}^{0.25}$, and we report the selection error rate as $\text{SR}(G) = K^{-1} \sum_{k=1}^K I(\hat{G}^{(k)} = G)$, where $\hat{G}^{(k)}$ maximizes the LIC in the k th simulation.

Summary statistics based on $K = 500$ simulation runs are given in Table 5, where we can see that even when G is over-specified, the consistency result still holds. For instance, PD_β drops from approximately 49.7×10^{-3} to 13.7×10^{-3} as (m, T) increases from $(100, 5\omega)$ to $(200, 10\omega)$

Table 5: Estimation accuracy and selection rate of G when G is misspecified.

		SBM network												Power Law network											
		$m = 100$						$m = 200$						$m = 100$						$m = 200$					
T	G	μ	β	η	γ	B	SR	μ	β	η	γ	B	SR	μ	β	η	γ	B	SR	μ	β	η	γ	B	SR
		$(\times 10^{-3})$					(%)	$(\times 10^{-3})$					(%)	$(\times 10^{-3})$					(%)	$(\times 10^{-3})$					(%)
5ω	2	396	86.3	254.2	384.7	120.0	1	387	83.7	234.8	352.1	108.2	0	409	88.2	263.4	398.0	121.2	3	383	85.5	248.1	349.0	113.7	0
	3	232	46.2	148.8	213.1	67.7	84	161	31.9	102.6	143.3	49.6	98	237	51.8	167.9	247.5	74.0	80	164	33.8	107.8	155.9	46.9	97
	4	252	49.7	161.2	229.4	68.3	15	178	46.1	149.2	221.9	61.7	2	261	60.4	192.2	275.2	81.7	17	182	39.7	126.5	181.5	53.9	3
	5	248	51.4	166.7	231.7	69.7	0	178	46.5	148.8	225.3	62.6	0	259	57.8	180.8	264.8	79.6	0	181	40.0	126.9	195.6	53.5	0
	6	252	49.2	163.3	225.0	68.9	0	178	45.9	148.3	224.5	62.3	0	261	57.7	182.5	270.4	80.1	0	181	40.3	127.2	179.2	54.3	0
	oracle	218	18.0	71.1	70.7	32.2	-	159	23.0	73.6	84.9	36.5	-	219	18.3	63.1	77.1	30.6	-	160	13.2	45.7	51.3	23.0	-
	10ω	2	374	83.6	240.1	383.5	115.8	0	333	82.6	226.9	408.0	110.7	0	387	83.1	240.2	370.2	113.1	1	384	82.6	235.5	377.1	111.3
3		161	15.1	55.6	54.9	28.5	96	123	9.4	32.2	34.7	19.1	99	162	17.1	60.7	74.7	32.7	91	125	10.5	38.8	43.7	20.0	98
4		173	20.6	71.0	70.7	31.1	4	132	13.7	43.9	45.7	20.7	1	172	24.6	81.0	102.4	37.5	8	135	16.2	53.1	69.2	25.2	2
5		183	24.7	85.3	102.5	35.8	0	146	17.0	52.3	56.2	26.1	0	183	31.6	101.8	136.9	45.9	0	150	20.5	63.4	82.3	30.0	0
6		190	28.3	95.5	120.7	40.7	0	153	21.1	65.5	74.7	29.4	0	192	37.8	126.0	171.8	54.2	0	159	23.2	75.2	92.2	33.7	0
oracle		160	12.4	44.0	42.9	19.8	-	123	8.9	29.1	31.5	16.2	-	160	13.3	45.3	52.8	21.8	-	124	8.8	30.4	34.5	15.2	-
20ω		2	353	81.9	232.7	389.1	115.1	0	320	83.9	240.6	417.8	114.7	0	357	81.5	230.1	387.0	112.0	0	360	82.2	230.8	392.2	111.3
	3	126	9.2	31.9	31.3	16.1	98	104	6.3	21.1	22.3	12.5	99	126	9.4	31.0	36.6	17.6	97	104	6.4	21.4	24.8	10.9	99
	4	132	11.6	41.2	40.2	18.2	2	109	8.5	28.6	29.3	12.9	1	132	13.2	43.0	50.4	21.5	3	111	9.2	29.1	33.9	14.5	1
	5	138	14.2	48.7	50.0	23.0	0	121	12.3	33.7	34.1	16.4	0	139	15.3	51.3	60.1	26.4	0	120	11.7	38.1	42.2	18.6	0
	6	141	15.5	54.4	59.6	24.7	0	124	12.2	40.3	40.8	18.1	0	143	20.4	66.4	80.3	32.2	0	126	12.9	41.3	48.7	20.1	0
	oracle	125	9.0	30.1	30.2	14.2	-	104	6.2	21.1	22.1	12.1	-	126	9.1	30.0	35.9	15.2	-	103	6.4	21.3	24.7	10.8	-
	40ω	2	339	82.2	237.2	401.7	118.0	0	245	110.0	372.5	550.9	117.2	0	346	80.5	227.4	395.9	112.7	0	363	81.1	225.0	392.1	110.0
3		104	6.5	22.5	21.9	11.8	99	92	4.7	16.6	18.2	9.0	100	104	6.7	21.6	25.5	12.9	98	90	4.6	15.9	19.2	10.2	100
4		108	8.2	27.6	28.7	12.7	1	97	5.7	20.9	23.8	8.9	0	109	8.5	28.2	34.5	15.0	2	96	6.1	20.9	24.8	10.2	0
5		111	9.3	33.4	33.5	15.1	0	100	7.0	24.6	27.0	11.9	0	112	10.6	33.1	41.8	19.3	0	100	7.6	25.1	30.6	13.1	0
6		112	10.5	36.8	38.3	16.6	0	103	8.3	27.6	30.2	12.7	0	114	12.4	41.4	51.6	22.6	0	103	8.7	30.0	33.4	14.2	0
oracle		104	6.3	22.3	21.8	9.8	-	92	4.7	16.3	18.1	9.0	-	104	6.5	20.9	25.0	10.7	-	90	4.5	15.7	19.2	10.1	-

with $G = 4$, which corroborates with the result in Theorem 2. When $G > 3$, estimation errors are generally larger than those of the case with $G = G_0$, which is reasonable due to the additional estimation variability introduced by an overly large G . Lastly, the proposed LIC can correctly select the true number of groups with a probability tending to 1 as (m, T) increases, which supports our conclusion of Theorem 5.

6 EMPIRICAL STUDY: A SINA WEIBO DATASET

We now apply the proposed GNHP model to a dataset collected from Sina Weibo, the largest Twitter type online social media in China. In this data set, we collect posting time stamps of $m = 2,038$ users from January 1st to 15th, 2014. Figure 4 gives two sample Weibo posts by James Cameron, where the posting times are highlighted in rectangles. The adjacency matrix

A of the network is constructed using the following-follower relationship observed among the users, and the resulting network density is $\sum_{i,j} a_{ij}/m(m-1) = 2.7\%$, suggesting a highly sparse network. Distributions of in-degrees and out-degrees of the network are given in Figure 4, where we can see that the in-degrees tend to be more skewed than the out-degrees. Such an observation is typical for a social network platform, where a few influential users may have a large number of followers but most users do not follow too many other users.

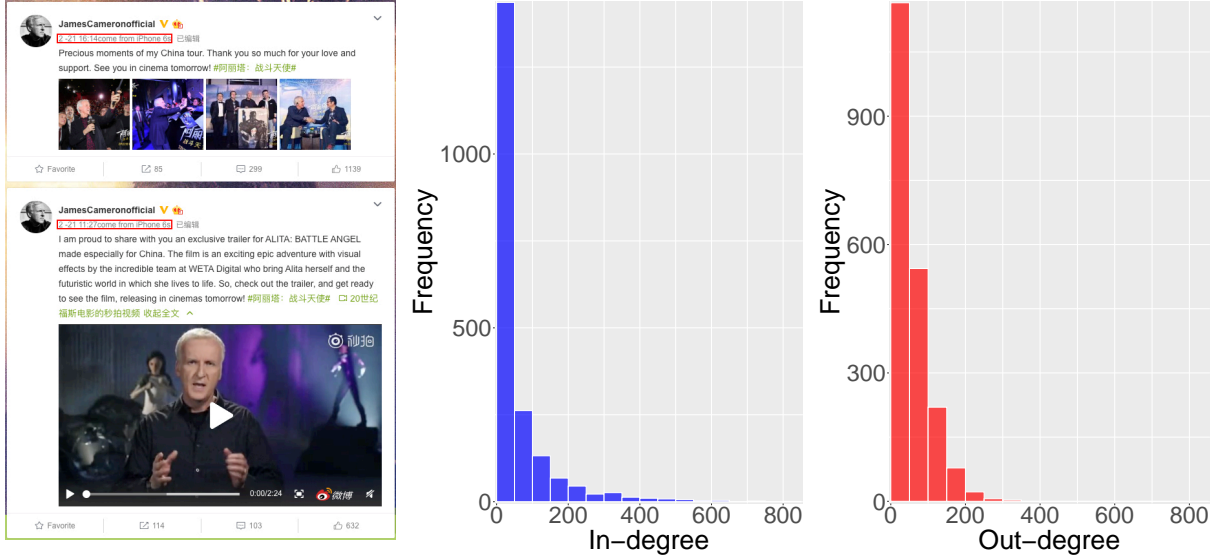


Figure 4: Left panel: A snapshot of James Cameron’s Weibo posts; Middle panel: histogram of in-degrees; Right panel: histogram of out-degrees.

6.1 Model Estimation and Interpretation

To estimate the GNHP model, we approximate the background intensities by B-spline basis with 8 equally spaced knots between 0 to 24 (hours) and the truncated exponential triggering functions (3) with $b = 5$ (hours). For better numerical stability, we put an upper bound 100 on parameters η_g ’s and γ_g ’s. Using the EM algorithm proposed in Section 3.3 with 200 initial membership and parameter estimates obtained from the algorithm in Section A.2 of the supplementary material, we first use the proposed LIC given in (19) to choose the number of latent groups with $\lambda_{mT} = (15T)^{-1} (\text{median}_{1 \leq i \leq m} n_i)^{0.6} \bar{d}^{0.25}$. From Figure 5, we can see that the log-

likelihood has a steep increase when G changes from 1 to 2, suggesting that it might be suitable to use a latent group structure to model the heterogeneity among the network nodes. The optimal number of groups chosen by LIC is $G = 4$, for which model the estimated background intensities are illustrated in Figure 5 and the resulting parameter estimates are summarized in Table 6.

Table 6: Parameter estimates for Weibo data (p-values are given in the parentheses).

Group (g/g')	Percent (%)	β_g		η_g		γ_g		$\phi_{gg'}$			
		-	-	-	-	-	-	1	2	3	4
1	52.6	0.342 (<0.001)	9.11 (<0.001)	1.47 (<0.001)	0.052 (<0.001)	0.110 (<0.001)	0.011 (<0.001)	0.027 (<0.001)			
2	23.3	0.318 (<0.001)	1.06 (<0.001)	2.33 (<0.001)	0.099 (<0.001)	0.181 (<0.001)	0.077 (<0.001)	0.005 (0.50)			
3	12.1	0.587 (<0.001)	0.69 (<0.001)	100 (<0.001)	0.011 (0.32)	0.059 (<0.001)	0.184 (<0.001)	0.003 (0.65)			
4	12.0	0.622 (<0.001)	6.27 (<0.001)	1.35 (<0.001)	0.075 (0.02)	0.298 (<0.001)	0.053 (<0.001)	0.186 (<0.001)			

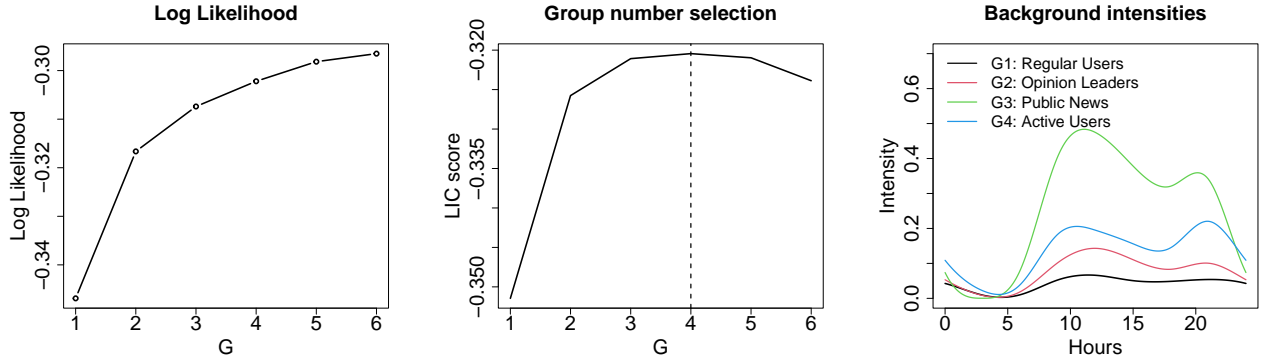


Figure 5: Left panel: maximized log-likelihood of various G 's; Middle panel: LIC scores of various G 's; Right panel: estimated background intensities.

As can be seen from Figure 5, the estimated background intensities all have two peaks around 10:00 am and 8:00 pm, suggesting that users are more active around these two time points. Based on the estimated GNHP model and users' information in the different groups, we categorize all users into the following four groups.

- Group 1. (REGULAR USERS). This is the largest group that includes 52.6% of users, who have the lowest background posting intensity throughout the day. Judging from $\hat{\phi}_{g1}$'s, users from this group have little impact on users from other groups. This group also has the largest $\hat{\eta}$ value, suggesting that the user's past posts have the shortest time impacts on his/her future posting behavior.

- Group 2. (OPINION LEADERS). This group mainly consists of users that are playing leading roles in various communities such as entertainment, business, education, and social sciences. They typically do not post very frequently throughout the day. This group has the second smallest $\hat{\eta}$ value, indicating that users' past posts have a relatively long time effect. From the estimated $\hat{\phi}_{g2}$'s, we can see this group of users have the largest impacts on all groups except Group 3. Our subsequent analysis reveals that this group is the second most influential group, see Section 6.2 for details,
- Group 3. (PUBLIC NEWS). Members of this group are mainly official accounts of some news outlets. Figure 5 shows that this group is the most active one on average, which is probably due to their mission to deliver information promptly. It has the smallest $\hat{\eta}$, suggesting the longest temporal dependence on the posting histories. At the same time, it has an extremely large $\hat{\gamma}$, which indicates that this group is very unlikely to be influenced by past posts from other groups. Although the estimated $\hat{\phi}_{g3}$'s are not as large as those of Group 2, the largest background intensity of this group makes it the most influential group, as we shall demonstrate in Section 6.2.
- Group 4. (ACTIVE USERS). This group consists of active users who post quite frequently as suggested in Figure 5. However, they have rather limited impacts on other groups based on the estimated $\hat{\phi}_{g4}$'s. It has a large $\hat{\phi}_{42} = 0.298$, indicating that users in this group are heavily influenced by users in Group 2.

6.2 Group Interaction and Influential User Analysis

In social network analysis, identifying influential users is an important task, as it may help improve the efficiency of news propagation, product release, and promotional campaign launches (Aral and Walker, 2011; Stephen and Galak, 2012; Zhu et al., 2019a). In order to identify the most influential users, we first define the influential power of the user i as the sum of the i th column of the matrix $(\mathbf{I} - \hat{\mathbf{B}})^{-1}$, which is the NODE-TO-NETWORK INFLUENCE given by Theorem

1. The bar plots of influential powers of the top 20 and top 100 influential users are illustrated in Figure 6. We can see that the top 20 influential users only consist of members from the “Opinion Leaders” group and the “Public News” group, with the latter group being the most influential one. This observation is further confirmed in the barplot of the top 100 influential users, where the majority of users are from Groups 2 and 3.

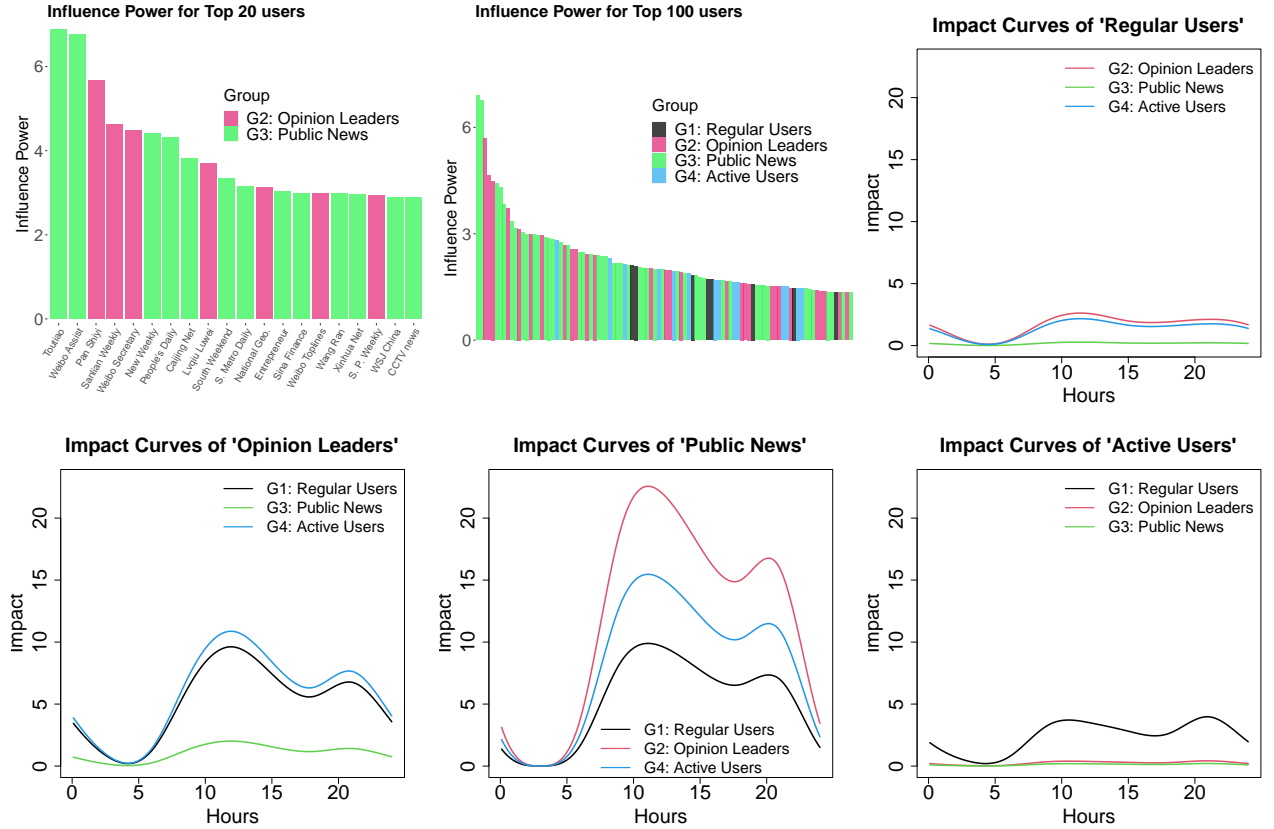


Figure 6: Barplot of top 20 and top 100 influential users.

To shed more light on the interactive relationships between the different groups, Figure 6 also gives impact curves of each group on the other groups as defined in (5). We can see that both the “Regular User” group and the “Active User” group have rather limited impacts on other groups throughout the day, which is as expected. It appears that the most influential group “Public News” has the largest impact on the “Opinion Leaders” group, indicating that users in the latter group may have the greatest need for timely news, which can be provided by users in the former group, so they could express their opinions following occurrences of news-worthy events. The

“Active Users” group is impacted more heavily than the “Regular Users” group by the “Public News” group, probably because users in the “Active Users” group are more active and hence can react to news more quickly than those in the “Regular User” group. Lastly, the impact of the “Opinion Leaders” group on the “Regular Users” group and the “Active Users” group are rather similar, an interesting phenomenon that may require a deeper look. Overall, the influence power plots and the impact curve plots reveal some interesting interactive patterns among social network users, which suggests the potential usefulness of the proposed GNHP model.

7. DISCUSSION

We propose a group network Hawkes process (GNHP) model that is suitable for analyzing the dynamic behavior patterns of heterogeneous users in a large network. The GNHP model extends the classical Hawkes model by utilizing the network structure and introduces a latent group structure to account for commonly encountered heterogeneity among network users. Theoretical properties of the proposed model are thoroughly investigated and a computationally efficient EM algorithm is proposed based on a novel branching process representation. The GNHP model is highly interpretable, as we have demonstrated through an application to a Sina Weibo dataset.

The proposed model is suitable for abundant applications such as epidemic studies (Wang et al., 2020), crime pattern analysis (Mohler et al., 2011), financial risk management (Zhu et al., 2019b; Chen et al., 2020), as long as the network structure can be identified. Several research topics can be pursued for future studies. First, the GNHP model can be modified to include covariates such as gender, region, user self-defined labels, longitudinal information (Blei et al., 2003; Shen et al., 2016; Xu et al., 2019). It will be even more challenging if the covariates are high-dimensional. Next, while we have only considered one type of user behavior, it would be interesting to incorporate multi-type user behaviors into the model for analyzing data collected from a social network with more complicated structures. Finally, the network structure in the current framework is assumed to be known and fixed. It is also of great interest to extend the current model to be suitable for networks whose topological structures are evolving over time.

References

- Achab, M., Bacry, E., Gaïffas, S., Mastromatteo, I., and Muzy, J.-F. (2018), “Uncovering causality from multivariate Hawkes integrated cumulants,” *Journal of Machine Learning Research*, 18, 1–28.
- Aral, S. and Walker, D. (2011), “Creating social contagion through viral product design: A randomized trial of peer influence in networks,” *Management Science*, 57, 1623–1639.
- Bacry, E., Bompairé, M., Gaïffas, S., and Muzy, J.-F. (2020), “Sparse and low-rank multivariate Hawkes processes,” *Journal of Machine Learning Research*, 21, 1–32.
- Bacry, E., Delattre, S., Hoffmann, M., and Muzy, J.-F. (2013), “Modelling microstructure noise with mutually exciting point processes,” *Quantitative Finance*, 13, 65–77.
- Blei, D. M., Ng, A. Y., and Jordan, M. I. (2003), “Latent dirichlet allocation,” *Journal of Machine Learning Research*, 3, 993–1022.
- Cai, B., Zhang, J., and Guan, Y. (2020), “Latent network structure learning from high dimensional multivariate point processes,” *Working Paper*.
- Chen, E. Y., Fan, J., and Zhu, X. (2020), “Community network auto-regression for high-dimensional time series,” *arXiv preprint arXiv:2007.05521*.
- Chen, S., Shojaie, A., Shea-Brown, E., and Witten, D. (2017), “The multivariate Hawkes process in high dimensions: Beyond mutual excitation,” *arXiv preprint arXiv:1707.04928*.
- Cohen-Cole, E., Liu, X., and Zenou, Y. (2018), “Multivariate choices and identification of social interactions,” *Journal of Applied Econometrics*, 33, 165–178.
- Farajtabar, M., Wang, Y., Gomez-Rodriguez, M., Li, S., and Zha, H. (2017), “COEVOLVE: A joint point process model for information diffusion and network evolution,” *Journal of Machine Learning Research*, 18, 1–49.
- Fleming, T. R. and Harrington, D. P. (2011), *Counting processes and survival analysis*, vol. 169, John Wiley & Sons.
- Fox, E. W., Short, M. B., Schoenberg, F. P., Coronges, K. D., and Bertozzi, A. L. (2016), “Modeling e-mail networks and inferring leadership using self-exciting point processes,” *Journal of the American Statistical Association*, 111, 564–584.
- Halpin, Peter, F., Boeck, D., and Paul (2013), “Modelling dyadic interaction with Hawkes processes,” *Psychometrika*, 78, 793–814.
- Hansen, N. R., Reynaud-Bouret, P., Rivoirard, V., et al. (2015), “Lasso and probabilistic inequalities for multivariate point processes,” *Bernoulli*, 21, 83–143.
- Hawkes, A. G. (1971), “Spectra of some self-exciting and mutually exciting point processes,” *Biometrika*, 58, 83–90.
- Hawkes, A. G. and Oakes, D. (1974), “A cluster process representation of a self-exciting process,” *Journal of Applied Probability*, 11, 493–503.

- Karrer, B. and Newman, M. E. (2011), “Stochastic blockmodels and community structure in networks,” *Physical Review E*, 83, 016107.
- Lee, L.-f. (2004), “Asymptotic distributions of quasi-Maximum likelihood estimators for spatial autoregressive models,” *Econometrica*, 72, 1899–1925.
- Linderman, S. and Adams, R. (2014), “Discovering latent network structure in point process data,” in *International Conference on Machine Learning*, pp. 1413–1421.
- Liu, R., Shang, Z., Zhang, Y., and Zhou, Q. (2020), “Identification and estimation in panel models with overspecified number of groups,” *Journal of Econometrics*, 215, 574–590.
- Liu, X. (2014), “Identification and efficient estimation of simultaneous equations network models,” *Journal of Business & Economic Statistics*, 32, 516–536.
- Liu, X., He, Q., Tian, Y., Lee, W.-C., McPherson, J., and Han, J. (2012), “Event-based social networks: linking the online and offline social worlds,” in *Proceedings of the 18th ACM SIGKDD international conference on Knowledge discovery and data mining*, ACM, pp. 1032–1040.
- Mohler, G. O., Short, M. B., Brantingham, P. J., Schoenberg, F. P., and Tita, G. E. (2011), “Self-exciting point process modeling of crime,” *Journal of the American Statistical Association*, 106, 100–108.
- Ogata, Y. (1978), “The asymptotic behaviour of maximum likelihood estimators for stationary point processes,” *Annals of the Institute of Statistical Mathematics*, 30, 243–261.
- (1988), “Statistical models for earthquake occurrences and residual analysis for point processes,” *Journal of the American Statistical association*, 83, 9–27.
- Phua, C., Lee, V., Smith, K., and Gayler, R. (2010), “A comprehensive survey of data mining-based fraud detection research,” *arXiv preprint arXiv:1009.6119*.
- Rasmussen, J. G. (2013), “Bayesian inference for Hawkes processes,” *Methodology and Computing in Applied Probability*, 15, 623–642.
- Sayyadi, H., Hurst, M., and Maykov, A. (2009), “Event detection and tracking in social streams,” in *Third International AAAI Conference on Weblogs and Social Media*.
- Shen, Y., Huang, H., and Guan, Y. (2016), “A conditional estimating equation approach for recurrent event data with additional longitudinal information,” *Statistics in Medicine*, 35, 4306–4319.
- Stephen, A. T. and Galak, J. (2012), “The effects of traditional and social earned media on sales: A study of a microlending marketplace,” *Journal of Marketing Research*, 49, 624–639.
- Su, L., Shi, Z., and Phillips, P. C. (2016), “Identifying latent structures in panel data,” *Econometrica*, 84, 2215–2264.
- Veen, A. and Schoenberg, F. P. (2008), “Estimation of space-time branching process models in seismology using an EM-type algorithm,” *Journal of the American Statistical Association*, 103, 614–624.

- Wang, L., Wang, G., Gao, L., Li, X., Yu, S., Kim, M., Wang, Y., and Gu, Z. (2020), “Spatiotemporal dynamics, nowcasting and forecasting of COVID-19 in the United States,” *arXiv preprint arXiv:2004.14103*.
- Wang, Y. J. and Wong, G. Y. (1987), “Stochastic blockmodels for directed graphs,” *Journal of the American Statistical Association*, 82, 8–19.
- Xu, H., Fang, G., and Ying, Z. (2019), “A latent topic model with markovian transition for process data,” *arXiv preprint arXiv:1911.01583*.
- Xu, H., Farajtabar, M., and Zha, H. (2016), “Learning granger causality for hawkes processes,” in *International Conference on Machine Learning*, pp. 1717–1726.
- Zarezade, A., De, A., Upadhyay, U., Rabiee, H. R., and Gomez-Rodriguez, M. (2018), “Steering social activity: a stochastic optimal control point of view,” *Journal of Machine Learning Research*, 18, 1–35.
- Zhang, C., Chai, Y., Guo, X., Gao, M., Devilbiss, D., and Zhang, Z. (2016), “Statistical learning of neuronal functional connectivity,” *Technometrics*, 58, 350–359.
- Zhao, Y., Levina, E., Zhu, J., et al. (2012), “Consistency of community detection in networks under degree-corrected stochastic block models,” *The Annals of Statistics*, 40, 2266–2292.
- Zhou, K., Zha, H., and Song, L. (2013), “Learning social infectivity in sparse low-rank networks using multi-dimensional hawkes processes,” in *Artificial Intelligence and Statistics*, pp. 641–649.
- Zhou, S., Shen, X., Wolfe, D., et al. (1998), “Local asymptotics for regression splines and confidence regions,” *Annals of Statistics*, 26, 1760–1782.
- Zhu, X., Chang, X., Li, R., and Wang, H. (2019a), “Portal nodes screening for large scale social networks,” *Journal of Econometrics*, 209, 145–157.
- Zhu, X., Pan, R., Li, G., Liu, Y., and Wang, H. (2017), “Network Vector Autoregression,” *The Annals of Statistics*, 45, 1096–1123.
- Zhu, X., Wang, W., Wang, H., and Härdle, W. K. (2019b), “Network quantile autoregression,” *Journal of econometrics*, 212, 345–358.